12-2011

Robust Design and Monitoring Tools for Sustainable and Resilient Structural Design and Infrastructure Management

Sarah Dalton
Clemson University, sarah.k.dalton@gmail.com

ROBUST DESIGN AND MONITORING TOOLS FOR SUSTAINABLE AND RESILIENT STRUCTURAL DESIGN AND INFRASTRUCTURE MANAGEMENT

A Thesis
Presented to
the Graduate School of
Clemson University

In Partial Fulfillment
of the Requirements for the Degree
Master of Science in
Civil Engineering

---

by
Sarah Katherine Dalton
December 2011

Accepted by:
Dr. Sez Atamturktur, Committee Chair
Dr. Hsein Juang, Committee Co-Chair
Dr. Weichiang Pang

ABSTRACT

Structural systems are subject to inherent uncertainties due to the variability in many hard-to-control *'noise factors'* that include but are not limited to external loads, material properties, and construction workmanship. Two design methodologies have been widely accepted in the practicing engineering realm to manage the variability associated with operational structures: Allowable Stress Design (ASD) and Load and Resistance Factor Design (LRFD). These traditional approaches explicitly recognize the presence of uncertainty; however, they do not take robustness against this uncertainty into consideration. Overlooking this robustness against uncertainty in the structural design process has two drawbacks. First, the design may not satisfy the safety requirements if the actual uncertainties in the noise factors are underestimated. Thus, the safety requirements can easily be violated because of the high variation of the system response due to noise factors. Second, to guarantee safety in the presence of this high variability of the system response, the structural designer may be forced to choose an overly conservative, inefficient and thus costly design. When the robustness against uncertainty is not treated as one of the design objectives, this trade-off between the over-design for safety and the under-design for cost-savings is exacerbated. The second chapter of this thesis demonstrates that safe and cost-effective designs can be achieved by implementing *Robust Design* concepts originally developed in manufacturing engineering to consider the robustness against uncertainty. Robust Design concepts can be used to formulate structural designs, which are insensitive to inherent variability in the design process, thus saving cost, and exceeding the main objectives of safety and serviceability. The second

chapter of this thesis presents two methodologies for the application of Robust Design principles to structural design utilizing two optimization schemes: *one-at-a-time* optimization method and *Particle Swarm Optimization (PSO)* method.

Next, this multi-disciplinary research project introduces a methodology to build a new framework, Structural Life-Cycle Assessment (S-LCA), for quantifying the structural sustainability and resiliency of built systems. This project brings together techniques and concepts from two distinct disciplines: Structural Health Monitoring (SHM) of Civil Engineering and Life Cycle Assessment (LCA) of Environmental Engineering to construct the aforementioned S-LCA charts. The intellectual innovations of this project lie in the advancement in infrastructure management techniques through the development of S-LCA charts, which can be useful as an infrastructure monitoring and decision-making tool, for quantifying the structural sustainability and resiliency of built systems. Such a tool would be of great use in aiding infrastructure managers when prescribing maintenance and repair schemes, and emergency managers and first responders in allocating disaster relief effort resources. Moreover, a quantitative, real-time evaluation of structural damage after a disaster will support emergency managers in resource allocation. The project integrates science based modeling and simulation techniques with advanced monitoring and sensing tools, resulting in scientifically defendable, objective and quantitative metrics of sustainability and resiliency to be used in infrastructure management.

DEDICATION

I would like to dedicate this work to my family and friends. Thank you for being my support system and always believing in me.

ACKNOWLEDGMENTS

This material is based upon work supported by the National Science Foundation under Grant No. 1011478. Any opinions, findings, and conclusions or recommendations expressed in the material are those of the author and do not necessarily reflect the views of NSF.

The author would also like to acknowledge Mr. Ismail Farajpour for the help he provided in the development of codes utilized in this research. Also, acknowledgments should be given to Mr. Ed Duffy of Clemson's Cyber Infrastructure Technology Integration (CITI) group for aiding in the debugging of codes in order to utilize the Palmetto High Performance Computing Cluster. Lastly, many thanks are extended to Drs. Sez Atamturktur, Hsein Juang, and WeiChiang Pang for their continued help and guidance through my Master's journey, they have taught me so much.

TABLE OF CONTENTS Page

LIST OF FIGURES

LIST OF TABLES

CHAPTER ONE

INTRODUCTION

The infrastructure in the United States is approaching, or has already passed, its design lifespan. The nation is at a turning point, where much of the infrastructure is in such disrepair it must be extensively retrofitted or reconstructed. This presents an interesting opportunity for infrastructure managers and designers to achieve sustainable and resilient designs. With planned retrofits, infrastructure managers have the chance to implement online monitoring techniques and develop new proactive maintenance schemes with updated technologies that promote life-long structural sustainability. While, with new construction, designers can embrace design methods, which promote resiliency to unforeseen factors, such as extreme forces. This thesis will explore both of these opportunities.

In Chapter Two, a structural design framework utilizing robust design principles will be formed. This framework aims to provide a design methodology that improves upon currently implemented strategies, such as ASD and LRFD, to directly include inherent uncertainties into the design process. In incorporating uncertainty, a resilient structure can be formulated, one that is designed to safely and efficiently resist a range of factors.

In Chapter Three, a novel, sustainable and proactive maintenance scheme and health index is discussed and developed, calling on principles from Structural Health

Monitoring and Life Cycle Analysis. The goal of this framework is to monitor the health and sustainability of an infrastructure system over its entire lifespan by periodically quantifying the system's health index and sustainability metric. This framework provides a quantitative value of the system's condition to infrastructure managers.

Chapter Four presents the main findings of this Master's thesis, while discussing lessons learned, and future work useful in improving upon the concepts and results developed and presented herein.

CHAPTER TWO

ROBUST DESIGN OPTIMIZATION TO ACCOUNT FOR UNCERTAINTY IN THE STRUCTURAL DESIGN PROCESS

1. Introduction

The root of the structural engineer's job is to systematically make decisions regarding design parameters. There are infinite possible design configurations to choose from with the goal of achieving a constructible, serviceable, safe, and cost-effective design. These goals are in and of themselves, competing objectives, in that the safest design is most likely not the most cost efficient. These conflicting objectives force designers to make trade-offs to meet as many design goals as possible. To further complicate the process, these decisions are all made under uncertainty.

The life-cycle of a structural system is plagued by uncertainty, from design through operation. Uncertainty manifests itself in many forms some of which entail (i) trying to predict the future or assume confidence in the past; (ii) statistical limits, in which designers use discrete samples to predict the behavior of a whole system; (iii) model limits, in which the structural model developed in design and analysis simplifies reality obviating higher level physics in the system; (iv) randomness, in which structural properties are not a single value as assumed, but rather the properties vary spatially; and (v) human error, encompassing mistakes made during the design, fabrication, and construction processes that alter the *true* design or analysis) [1]. The inherent variability in these factors must be accounted for during the design process to ensure the proposed design objectives are met under all circumstances of interest.

Two prominent design approaches have evolved in the structural engineering field to account for the variability in design parameters. The first, allowable stress design (ASD), which originated in the 1920's, is based upon a deterministic design approach. Through the ASD approach, designers do not try to quantify the different sources of uncertainty, but, rather, apply a single subjective 'factor of safety' to capture *all* the variability in loads and resistance. The result is usually a conservative and safe design, but one, that is likely to be inefficient and over-designed [2]. The second approach, load and resistance factor design (LRFD), developed in the 1980's, is a form of reliability-based design. Here, uncertainties in the design process are quantified into two categories; nominal capacities and load and resistance factors. This separation allows for predictability of material properties and construction tolerances through nominal capacities, and predictability of variable loads through load and resistance factors. While this method accounts for variability and incorporates risk assessment, the success of the LRFD approach hinges on the availability and accuracy of statistical data [3]. In reliability-based designs, uncertainty is modeled as random variables or processes. If there is an abundant amount of accurate statistical data, and the distributions of each random variable is well established, then uncertainties can be accurately accounted for in the design. However, if there is a lack of statistical data and the distributions of parameters are not fully understood, resulting in poor estimation, then the random variables themselves induce uncertainties into the design process [3]. Therefore, the safety requirements might be violated due to the potentially underestimated variability in the structural behavior.

An alternative approach, Robust Design processes, originated in Manufacturing Engineering and employed in this chapter, target the robustness of the product output against “hard-to-control” input parameters (called “noise factors”), by adjusting “easy-to-control” input parameters (called “design parameters”) [4-5]. In the design of a concrete frame building (used as an example throughout this chapter), the column dimensions and the stiffness of the bracing elements may be treated as design parameters; the uncertain material properties or the forcing functions may be treated as noise factors; and the structural response such as, stresses, strains and displacements, may be treated as the product of the design process. Since these noise factors represent hard-to-control parameters, one cannot reduce or eliminate them in any feasible way. The aim should then be to reduce the effects of these noise factors on the structural response. This is precisely the purpose of Robust Design principles. By exploiting the non-linear interactions between the design parameters and the noise factors, Robust Design aims to find design parameters that yield a structural design which is robust to the hard-to-control noise factors, thereby reducing the variability of the structural response and yielding not only safe but also cost-effective designs.

Focusing on a concrete-frame model, this chapter demonstrates the feasibility and applicability of robust design principles in structural engineering. Herein, the principles of robust design are implemented through two distinct optimization methodologies: *Coordinate Descent* optimization method and *Particle Swarm Optimization (PSO)* method. Section Two of this chapter overviews the genesis of Robust Design principles as well as work completed to improve upon it. Section Three follows with the

methodologies used in this chapter to apply the Robust Design principles to our problem and finally, in Sections Four and Five, results and discussion for each of the optimization cases, respectively, will be presented.

2. Background

To reiterate, the goal of robust design is to manipulate easy-to-control parameters (design parameters), those parameters that the designer has the ability to manipulate, such as material type or geometric dimensions, to minimize the effects of hard-to-control control parameters (noise factors), such as construction imperfections or material variability, making the process more robust against noise and improving quality, and reliability at low costs [6, 4]. This process utilizes interactions between design parameters and noise factors to identify the design parameter settings, which reduce the effects of noise on the desired outcome the most *by reducing variability and adjusting the mean to a target value* [7-8]. This goal can be reached in several ways through utilizing the traditional two-step methodology as outlined by Taguchi [7], Bayesian Inference techniques [9], the multi-objective optimization techniques [10,11], or through a single-objective robust optimization scheme [10,11].

Taguchi [7] developed a two-step process for Robust Design (Figure 1.1). The first step focuses on minimizing the variation. This step seeks the optimum settings of the design variables by maximizing what Taguchi coins the *signal-to-noise (S/N)* ratio, defined as the ratio of response to the variation in response caused by noise factors. Three different classes of S/N ratios are defined. The first is *nominal-the-best*, where a

certain target value is desired. Second is *smaller-the-better*, where the most robust option is a zero value response, and likewise, the third class of S/N ratios, called *larger-the-better*, which ideally aims to achieve a target value of infinity. Equations 1.1-1.3 summarize the different classifications of S/N ratios, respectively, where μ is the mean of the system response, σ is the standard deviation of the response due to noise, and y_i are observed responses [12].

$$\eta = 10\log_{10}\left(\frac{\mu^2}{\sigma^2}\right) \tag{1.1}$$

$$\eta = -10\log_{10}\left[\frac{1}{n}\sum_{i=1}^{n} {y_i}^2\right] \tag{1.2}$$

$$\eta = -10\log_{10}\left[\frac{1}{n}\sum_{i=1}^{n} \frac{1}{{y_i}^2}\right] \tag{1.3}$$

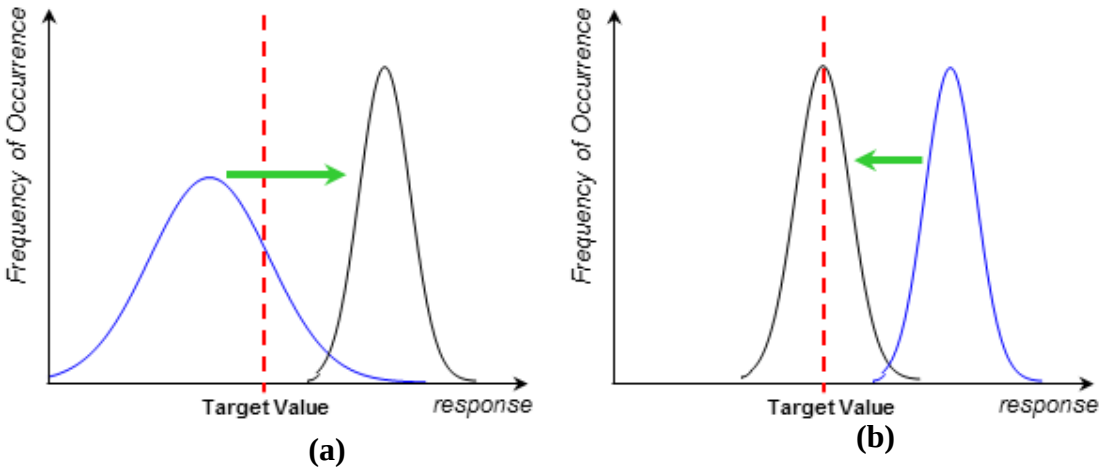

Figure 1.1: Two-step robust design methodology; (1a) minimize variability by altering design parameters (1b) move mean of distribution on target through the application of a scale factor

The second step of Taguchi's method focuses on moving the mean to the desired target (Figure 1.1). This can be accomplished through the careful selection of a design parameter(s), which affects *only* the mean of the distribution and illustrates no influence

on the variation of the distribution, while preserving the maximized signal-to-noise ratio achieved in step one. This design parameter(s) is considered a scale factor used to *scale* the mean to a desired value and can be calculated according to Equation 1.4 where *s* is the scale factor, *m* is the target value, and μ is the mean of the current distribution.

$$s = \frac{m}{\mu} \tag{1.4}$$

Taguchi first developed this methodology for process design, i.e. design of experiments, and not for product design. Due to its simplicity and proven advantages, the Taguchi method has been applied to various aspects of engineering [14-20]. In the adaptation of the principles of Taguchi's method for other engineering applications, several problems were encountered, which led to subsequent research and updated methods [11]. Some of these problems include the inability to locate a scale factor [21-23], high computational effort needed to gain insight into all factor interactions [24-26], and the inability of the method to include design constraints [12, 27-29]. Of these, the most widely studied is the lack of a scale factor.

There are practical design situations where all parameters significantly affect both the mean and standard deviation, proving the isolation of a single parameter which affects only the mean impossible. In such situations, Taguchi's two-step method is no longer applicable because the maximized signal-to-noise ratio is not upheld thereby causing an unintentional coincident shifting of the standard deviation in step two [7, 13]. In these instances, optimization methods [10-11, 36] or Bayesian inference [37-39] techniques can be employed to obtain design parameters while simultaneously considering the mean and standard deviation of the response.

3. Robust Structural Design Methodology

This thesis presents a simulation based proof-of-concept case-study, which seeks to find a structural design that is robust against noise factors given certain performance and cost constraints.

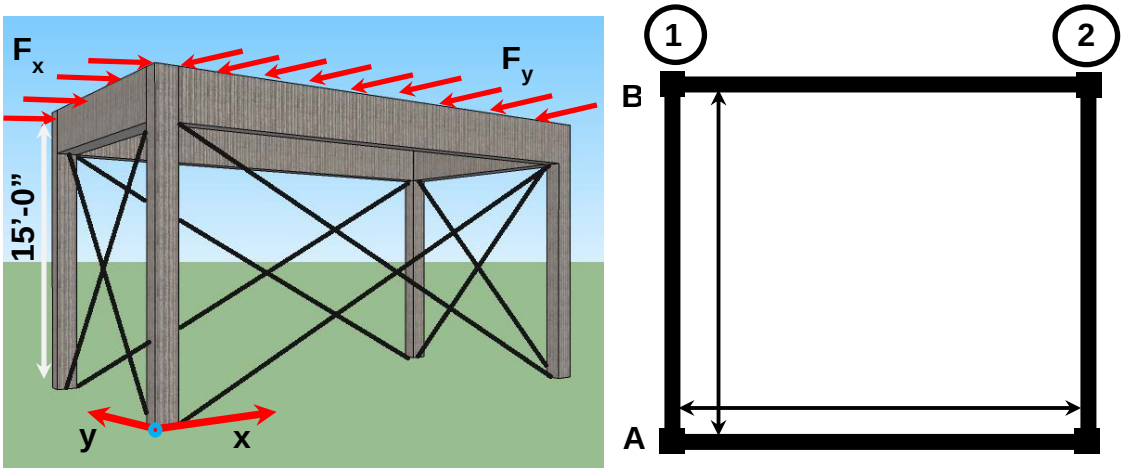

Figure 1.2: Basic prototype geometry and boundary conditions – left elevation, right plan view

3.1 Prototype Structure and Robust Methodology

For this proof-of-concept study, a one-story, one-bay, reinforced concrete frame structure with steel cross-bracing was chosen as the prototype. The geometry of the structure can be seen in Figure 1.2. A preliminary structural design for the frame was completed in accordance to ACI 318-08: Building Code Requirements for Structural Concrete and Commentary Standard, 2008 version using the recommended design loads.

In the first step of Robust Design methodology, **design constraints**, **design parameters**, **noise factors** must be defined and the ranges in which these parameters may vary must be determined.

The system response of interest is the drift of the structure under lateral load. The **design constraint** is set to be a *threshold value* for maximum drift in any horizontal direction at column B2.

In the structural design context, easy-to-control design parameters include geometric and member dimensions and material strengths. Herein, eight **design parameters** are employed for both optimization cases: (1) width of columns, X, (2) depth of columns, Y, (3) dimensions of the floor plan, L and W, (4) cross-sectional area of the bracing in the x-plane, A_x, (5) cross-sectional area of the bracing in the y-plane, A_y, (6) height of the beams, h_b, (7) strength of concrete, f_c', and (8) column reinforcement ratio, ρ. To observe design trade-offs between safety and cost-efficiency, as a practicing structural engineer would, a realistic structure with sufficient numbers of design parameters to manipulate is necessary. The lateral forces are applied in both x and y directions, making a larger number of design parameters influential on the maximum drift of the structure. The applied force in the x-direction is assumed to be twice that in the y-direction; however the procedure can easily be modified to implement other load scenarios. Since the geometric floor plan of the structure (L and W) is a design parameter, applied load is scaled to ensure the concentrated point load of the distributed pressure was constant for all design configurations.

Though a single **noise factor**, variability in distributed force at the roof level, is considered, the procedure can easily be extended to consider multiple noise factors as outlined in the introduction. The range of force values explored in this chapter represent a worst case scenario in the magnitude of force applied, i.e. natural hazard or blast

loadings. The force that causes the preliminary structure to enter its nonlinear realm is found and set as the upper bound. Thus the static force range explored herein ranges from 10,800 psf to 17,333 psf. These bounds are defined based on engineering judgment; whereas in real life, probabilistic analysis of the forces would be necessary to define such plausible bounds.

Table 1.1: Design parameters and their constraints

Parameter	Range of Acceptable Values
Width of Columns (X)	6 in – 24 in
Depth of Columns (Y)	6 in – 24 in
Floor Plan Dimensions (L and W)	Square Footage ~400ft^2 (L*W=400)
Area of Bracing in x plane (A_x)	0 in^2 – 8 in^2
Area of Bracing in y plane (A_y)	0 in^2 – 8 in^2
Height of Beams (h_b)	12 in – 36 in
Strength of Concrete (f_c')	2500 psi – 5500 psi
Column Reinforcement Ratio (ρ)	0.01 – 0.08

Much consideration is put into ensuring the resulting optimal designs are both feasible to construct and allowable by ACI building codes. Thus, design constraints, seen in Table 1.1, are imposed on the candidate designs. The design objective for this study is to achieve robustness for the drift of column B2 when exposed to uncertainty in the loading at roof level along members A1-A2 (in the y-direction) and A1-B1 (in the x-direction) (See Figure 1.2). To achieve the stated objective function, a defined threshold for drift values was also specified to be no more than 0.048 feet (0.575 inches) on a 15 foot tall structure. It should be noted that this threshold is not the value at failure, rather has a factor of safety applied to ensure the safety of the structure's users.

As robustness, in the most theoretical sense, also promotes efficiency, a secondary goal is to optimize for cost. For the purposes of this research, cost is defined as in Equation 1.5 where V_c is the total volume of concrete, V_s is the total volume of steel

bracing, and □ is the unit price of each material. The unit price for steel is assumed to be five times that of concrete [41]. Steel rebar and structural steel connections are included in their respective unit prices.

$$Cost = \sum V_c * \phi_c + \sum V_s * \phi_s \quad (1.5)$$

To achieve cost-efficiency, a secondary threshold representing cost is specified to be 500 unit price. Such constraint reduces the member dimensions of selected, plausible designs to only cost effective designs.

3.2 Development of Robust Objective Function

In the case study structure studied herein, Taguchi's two-step design process proved inapplicable due to the absence of a scaling factor [17]. This was due to the design parameters influencing both the mean and the variability of the response simultaneously. For instance, Figure 1.3 shows the effect of changing the width of columns (parameter *X*) on the drift value while keeping all other design parameters constant. For each design case presented in Figure 1.3, a maximum force level of 13,200 psf and minimum force level of 12,000 psf are imposed on the system and maximum drift at Column B2 is calculated for each of the two levels. The mean drift value for each design case is plotted in Figure 1.3 along with the variability in the calculated drift values. As visually observed, this design parameter significantly influences both the mean and variability.

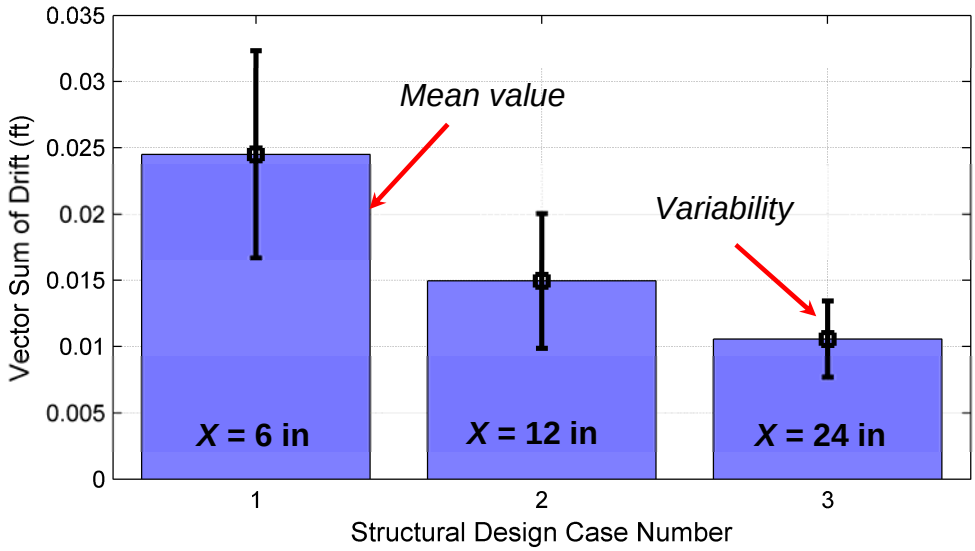

Figure 1.3: Effect of altering the width of columns on the objective

Solely by changing the width of the columns, the mean of the distribution is dropped from 0.0246 ft. for Design Case 1 to 0.0105 ft. for Design Case 3. This is a 57% decrease in the mean value. Concurrently, the range, which is representative of the sensitivity of this particular noise factor (i.e. force level), is dropped from 0.00787 ft. to 0.00295 ft., a 63% change. From these values it is clear that by altering the column width, *both* the mean and standard deviation of the drift value distribution are significantly affected. This observation holds true for all design parameters in this study proving Taguchi's two-step robust design is not a plausible option for this problem. In this case, the use of signal to noise ratios (Equations 1.1-1.3) is inappropriate because a change in S/N can be attributed to robustness to the noise factor or the interaction of the design parameters on both the mean and standard deviation. The alternative approach is then to seek a design in a single step where both the mean and standard deviation must be evaluated simultaneously.

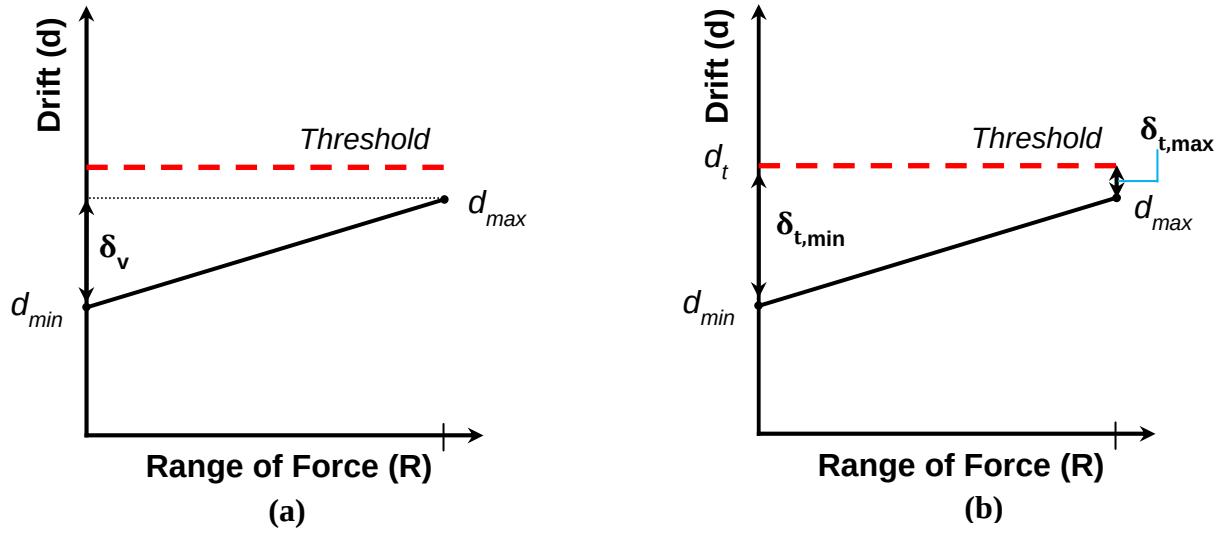

Figure 1.4: Robust optimization methodology - (a) reduce variability (b) reduce distance from threshold

If we can conceptualize a graph sorted with noise levels (force values) on the x-axis, and system response (maximum drift) on the y-axis, as seen in Figure 1.4, designs exposed to uncertainty can be represented by a single line connecting the drift values at each noise level, henceforth referred to as *system response curve*. The ideal robust design is then defined as a line with a slope of zero (i.e., infinite robustness), meaning there is no change in the system response over all noise levels, located precisely at a desired threshold level.

In the pursuit of such a response, this research calls upon the two-step robust design methodology to define a single objective robust optimization problem. After the establishment of a system response threshold, the first step is to minimize the variability in response by seeking a design with a slope, which approaches zero, implying a robust design. This can be accomplished in the framework of this research by minimizing the distance between d_{min} and d_{max}, δ_v in Figure 1.4a. The next goal is to avoid overdesign by

selecting one with a system response curve as close to the target threshold as possible without exceeding it. This can be accomplished by minimizing the distance between d_t and d_{min} ($\delta_{t,min}$) and d_t and d_{max} ($\delta_{t,max}$) in Figure 1.4b, ensuring the curve approaches the threshold. Thus, a robust optimization, which aims to instantaneously minimize δ_v, $\delta_{t,min}$, and $\delta_{t,max}$ can be accomplished by altering design parameters within their allowable domain to minimize the ***area*** between the defined threshold and the system response curve (A_R). In doing so, any need for a two-step process is obviated.

The calculated area (A_R) will be both problem and unit specific making it difficult to meaningfully compare parameter to parameter, or application to application. Thus, to put the calculated area into an understandable and comparable value, a Sensitivity Index (S_I) is developed. Here, A_R is compared to the entire area under the threshold to develop an index where a zero value represents an infinitely robust and insensitive system at the desired threshold, and a value of one represents an infinitely robust system with essentially no response, i.e. a very costly design. With this reasoning, a small Sensitivity Index is desired, the goal of which is to find a design that is insensitive to noise factors and is structurally efficient (having a system response closest to the threshold). This can be expressed mathematically through Equation 1.6 for a system with two noise levels. If a system response at multiple levels of noise factors is available, then the calculation of the S_I can be expanded to *n* levels by segmenting the system response curve to yield Equation 1.7. Herein, since multiple noise factor levels are evaluated, Equation 1.7 will be employed to quantify the robustness of designs, as defined in this research.

$$S_I = \frac{\delta_{t,min} + \delta_{t,max}}{2d_t} \tag{1.6}$$

$$S_I = \frac{\sum_{i=1}^{n} R_i\left(\frac{\delta_{t,min,i} + \delta_{t,max,i}}{2}\right)}{R \cdot d_t} \tag{1.7}$$

3.2 Prototype Structure Finite Element (FE) Formulation

A numerical model of the prototype structure, described in Section 3.1 of this chapter, was developed using the commercial FE modeling package, ANSYS version 13.0. To simulate the complex nonlinear behavior of concrete, Solid65, a dedicated solid isoparametric element, is utilized. Solid65 is a three-dimensional brick element with eight nodes, each allowing three translational degrees of freedom in the global x, y, and z directions [42]. As seen in Figure 1.5, a multilinear constitutive material model based on the triaxial behavior of concrete developed by William and Warnke is used to simulate failure [43]. The concrete is capable of cracking in three orthogonal directions, plastic deformation, and creep; however, in order to achieve convergence, crushing capabilities are turned off. This element is particularly suitable for our application due to its ability of incorporating reinforcement bars directly into the element through a smeared cross-section, thereby increasing the computational efficiency of the simulation. The rebar modeled in Solid65 is capable of tension, compression, plastic deformation, and creep.

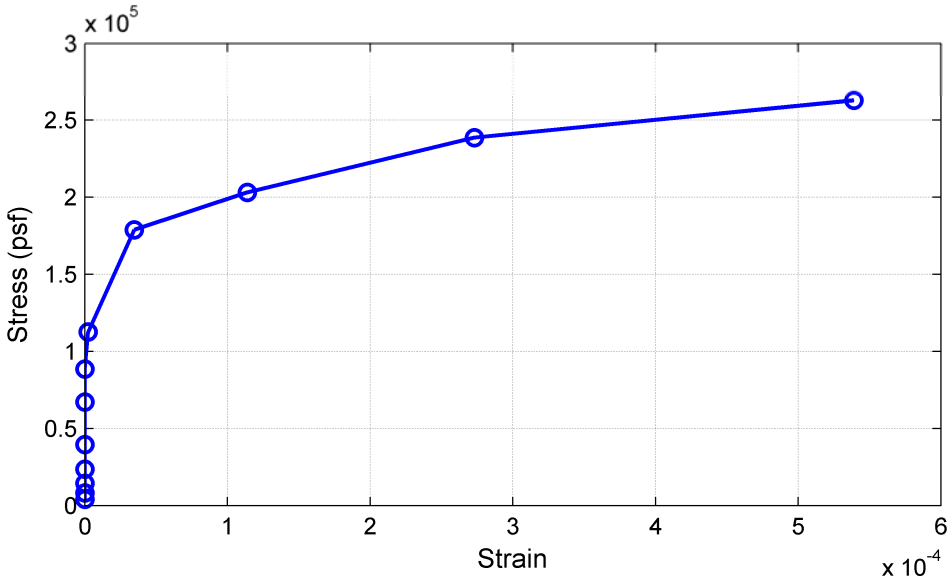

Figure 1.5: Concrete material model

3.3 Simulation Campaign

Five hundred designs, each with four noise levels, are simulated for use in both optimization methods which are discussed in the next two sections. Latin-hypercube design, a sampling method developed at Los Alamos National Laboratory, is used to sample the design domain in order to create these 500 hundred designs. This sampling method is advantageous in that it ensures an adequate coverage and exploration of the 8-dimensional design domain defined by eight design parameters (See Table 1.1).

4. Robust Structural Design Case Study – Coordinate Descent Method

4.1 Coordinate Descent Optimization Method

The Coordinate Descent Method, also known as the *one-at-a-time* optimization algorithm [44,45], minimizes the objective function by solving a series of scalar

minimization sub-problems. Each sub-problem minimizes along a certain coordinate, while all other coordinates remain constant [46]. The objective function can be defined as ω, defined in Equation 1.8 as:

$$\omega = Minimize(x_1, x_2, x_3, \cdots, x_n) \tag{1.8}$$

The minimization of ω is achieved by the sequential variation of one variable at a time while all others are fixed at their nominal values. At the first iteration of the algorithm, all variables are held constant with the exception of the first parameter (x_1). A new value is found for this variable which reduces the objective function. Upon the completion of this step, the first variable becomes fixed and the algorithm moves onto the second variable (x_2). This parameter is then varied until a new value that reduces the objective function is found. This process is followed for *n* iterations, where afterwards, the process returns to the first variable and the cycle is repeated until the solution converges to an optimal value [45].

In the context of this research, the objective function used herein is expressed by Equation 1.9.

$$\omega = Minimize(\delta_v + \delta_{t,min} + \delta_{t,max}) \tag{1.9}$$

Because all three parameters in the objective function are dependent upon the eight design parameters and the selected noise factor, the objective function is also dependent upon the design parameters outlined in Table 1.1 (X, Y, L and W, A_x, A_y, h_b, f_c`, ρ)and the noise factor.

The basic framework of this optimization algorithm, as applied to this research, is shown in Figure 1.6 where *x* are design values (x_0 are the preliminary values), *Δx* is the step size for the adjustment in each design parameter's value (for example column dimensions are designed on an integer basis, such as even inch dimensions, for constructability purposes), *ω(x)* is the objective function, *k* is a counter for the number of iterations operated on a singular parameter before the algorithm takes its current optimized value and moves onto the next parameter, and *i* is a counter for the number of design parameters to be optimized. To initiate the algorithm, a preliminary design, step size, and objective function are selected, and the counter variables are set to one. The drift, using the FE model, and objective function, using the algorithm, are calculated. The first parameter is then altered through a single step along the design parameter's coordinate, while all others remain fixed; the objective function is then calculated with the adjusted value. If this value is less than the preliminary design's objective function, the optimized

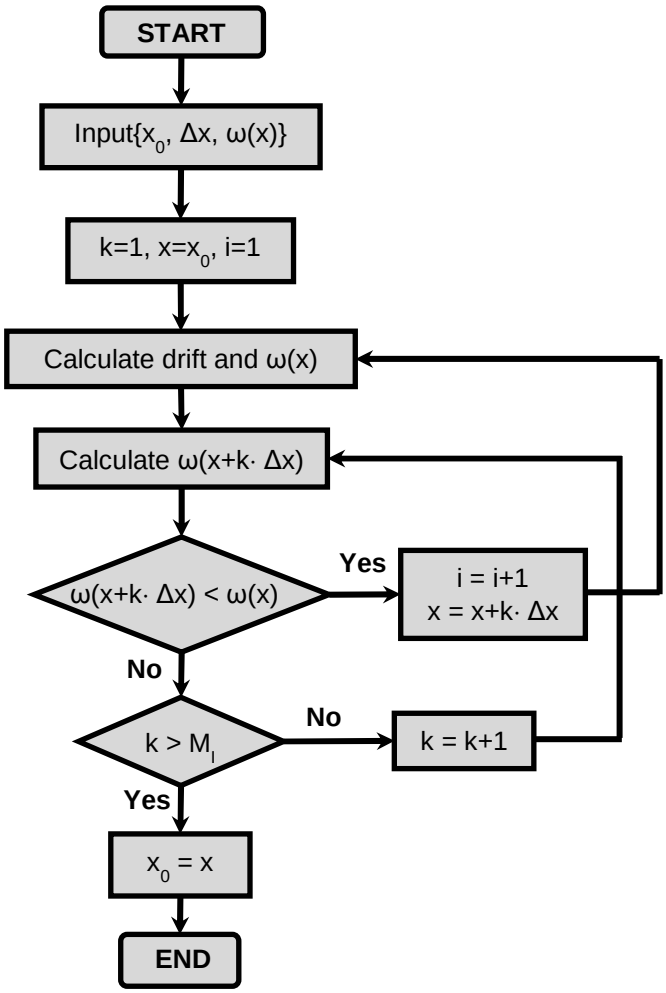

Figure 1.6: Coordinate Descent Method algorithm

value for design parameter one is taken, and fixed. The algorithm then moves onto the second parameter, repeating the process. If the optimized value for the first design parameter is not less than the preliminary objective function, another step is taken along the coordinate of the first design parameter and a subsequent objective function calculation is performed. This value for the objective function is again compared to the preliminary value and if improved, the optimized value is taken and fixed, and the algorithm moves onto the next design parameter. If there is improvement, another step is taken. This process is completed for all eight design parameters yielding a more optimal design. Upon completion, a new iteration can begin, the preliminary design parameter values of which become the optimized values from the previous iteration and the procedure outlined above is repeated. For this research, one iteration was completed with a k value equal to 10.

4.2 Coordinate Descent Optimization Results and Discussion

To compare the performance of the proposed Robust Structural Design, a nominal design is defined. The nominal case is specified to be the mean value of each of the eight design parameters' domains and is one of the many possible designs that satisfy the code requirements. The values for each of the eight nominal design parameters are outlined in Table 1.2.

The initial design parameter settings for the optimization algorithm are taken to be the design parameter settings from the 500 preliminary FE simulations which minimize the Sensitivity Index the most. For this case study, one Coordinate Descent Method iteration with four noise levels is completed on each of the eight design parameters to

find two robust designs (See Table 1.2), one which only minimizes the Sensitivity Index (option A) and a second which concurrently minimizes the Sensitivity Index and cost (option B).

The Sensitivity Index, which is 0.450 in the nominal design case, is reduced significantly by both approaches. The S_I decreased to 0.234 (48 percent decrease) in option A, and to 0.297 (40.67 percent decrease) in the option B, as it can be seen graphically in Figures 1.7 and 1.8.

Furthermore, to compare the efficiency of these alternative designs, the unit price of each design is computed. As expected, the design obtained in option A, which does not consider cost in the objective function, is found to increase robustness, but with the trade-off of increased cost. This design is found to be the most robust, but with a concurrent cost of 596 units, which are 139 units more expensive than the nominal design. Conversely, option B, which accounts for not only the Sensitivity Index but also the cost in objective function, yields an improvement in both the robustness and the efficiency of the design. This design is priced 11 units less than the nominal design, with 446 units. This observation illustrates that increased robustness can be achieved at reasonable cost (and even reduced cost), thus proving the practical applicability of the Robust Design methodology to structural engineering.

Table 1.2: Comparison of nominal and robust design parameters

	Nominal Design Values	Robust Design Values (Cost Not Considered)	Robust Design Values (Cost Considered)
Width of Columns (X)	15 inches	12 inches	15 inches
Depth of Columns (Y)	15 inches	18 inches	18 inches
Floor Plan Dimensions (L and W)	20 ft by 20 ft	22 ft by 18 ft	24 ft by 17
Area of Bracing in x plane (A_x)	4 in^2	1.25 in^2	2.60 in^2
Area of Bracing in y plane (A_y)	4 in^2	7.75 in^2	7.75 in^2
Height of Beams (h_b)	24 inches	45 inches	18 inches
Strength of Concrete (f_c`)	4000	3750	4250
Column reinforcement ratio (ρ)	0.045	0.08	0.025
Sensitivity Index	0.450	0.234	0.267
Cost of design	457 units	596 units	446 units

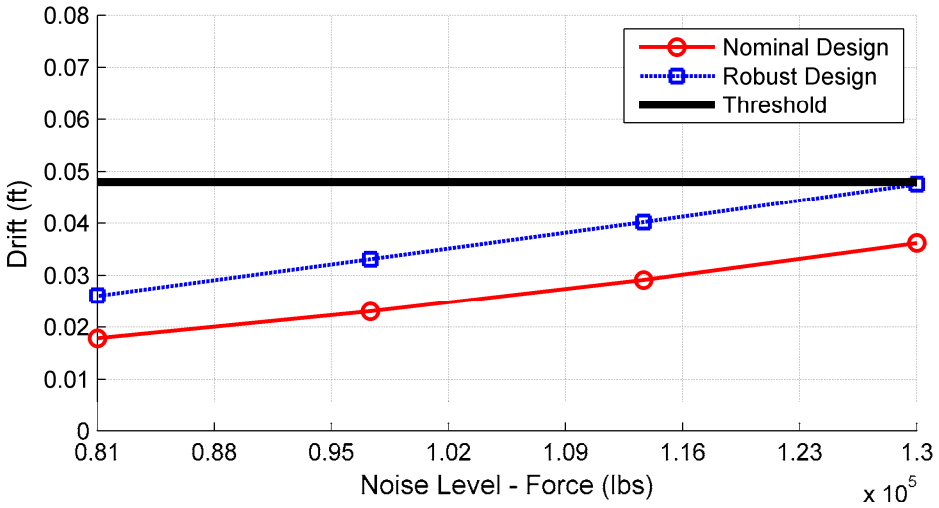

Figure 1.7: Graphical depiction of objective function for nominal and robust design cases, cost not considered

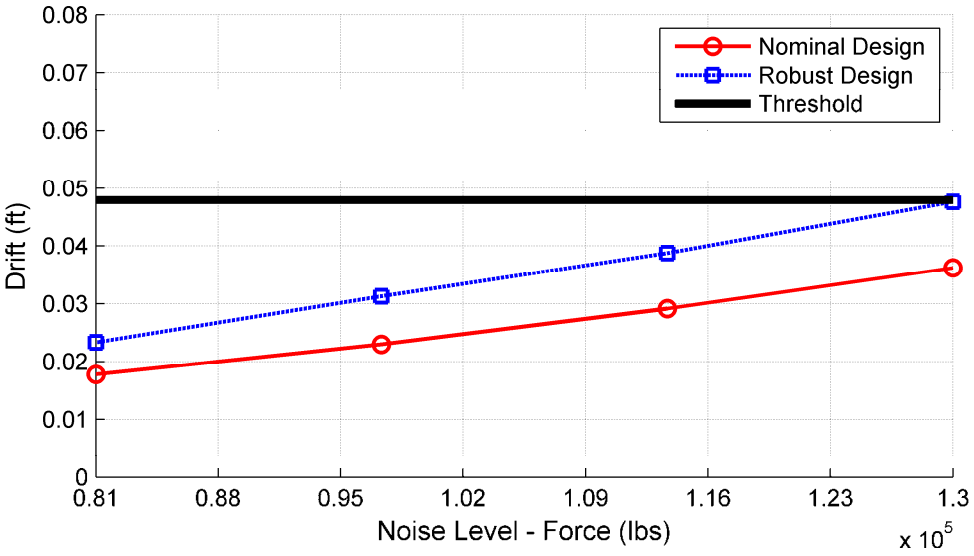

Figure 1.8: Graphical depiction of objective function for nominal and robust design cases, cost considered

5. Robust Structural Design utilizing Particle Swarm Optimization

5.1 Particle Swarm Optimization Method

To achieve the desired objective of maximizing robustness while maintaining safety and minimizing cost, a more detailed study is conducted utilizing the Particle Swarm Optimization (PSO) method. This method is a probability-based search algorithm initially developed by Eberhart and Kennedy [48], which falls under the swarm intelligence category of optimization algorithms [49]. The observed behavior of the instinctive movement of an animal to find food sources motivated the development of this method [50]. Using biological nomenclature as inspiration, the population is defined as a swarm and each individual within the swarm is called a particle. In order to control the distance a particle will travel in a single iteration of the process, PSO uses three

parameters, swarm size, social acceleration coefficient, and cognitive acceleration coefficient to reach a local minima [48]. The utilization of PSO is advantageous in this research due to its well-suited nature for the nonlinear and discontinuous domain ([51]) observed in the research problem presented in this manuscript.

Similar to the case-study presented in the previous section, interval analysis was used to keep computational costs due to simulations at a tractable level. The input-output relationship between the response of the structure and the input parameters is represented by a fast running 'response surface function', also known as an emulator or surrogate model. A matrix function is used to train the response surface to the FE simulated data and is used in place of the computationally expensive FE model. This response surface can, within reason, accurately predict the outcomes of all possible design configurations (within the defined ranges for the design parameters), at a computationally efficient manner. The response surface is a function of the eight design parameters: column width, column depth, floor plan dimensions, cross-sectional area of bracing in the x plane, cross-sectional area of bracing in the y plane, height of beams, strength of concrete, and reinforcement ratio. Through the use of a fast running emulator, a more continuous design domain is established at a computationally tractable manner, allowing the most robust design to be established within the definitions presented in this chapter.

Using this response surface, the objective is then to minimize the Sensitivity Index, i.e. the area between the specified drift threshold (that is constant for all noise levels presenting infinite robustness, in the most ideal case) and the performance of alternative designs for varying noise levels, as depicted in Figure 8. Therefore, the PSO

algorithm operates on minimizing this Sensitivity Index which is symbolically expressed in Equation 1.10.

$$\omega = Minimize(\delta_v + \delta_{t,min} + \delta_{t,max}) \quad (1.10)$$

5.2 Optimization Results and Discussion

In this section, the search for robust and cost-efficient design is undertaken through the PSO algorithm. A swarm size of 25, social acceleration coefficient of 1.3, and a cognitive acceleration coefficient of 2.8 are used in the PSO algorithm. These values are recommended values which keep run times to an efficient level and have been proven to avoid the possibility of the algorithm getting stuck at a local optima [52]. As discussed in Section 4.2, to achieve the stated robust design definition, cost must be an integral component of the objective function. Therefore, in this section, only option B where cost is considered is evaluated. The resulting robust design is outlined in Table 1.3.

Similar to the previous case study, the obtained robust design is compared to the nominal design defined by the mean values of each of the eight design parameters. Through the obtained robust design minimizes the Sensitivity Index by 65.8 percent, there was a slight cost increase of nine percent. For some building owners, this small increase in price may be acceptable in that the return-on-investment for the small increase in cost is offset by the substantial increase in robustness. The reduction in the Sensitivity Index is illustrated in Figure 1.9. Not only is the Sensitivity Index minimized for the robust design case, pictured as the dashed line with circular markers, but it is also very robust at high noise levels, exploiting the highly nonlinear design parameter and noise

relationship. As seen, the resulting design maximizes its insensitivity to noise factors, while simultaneously ensuring that the design cost stays within an efficient region.

Table 1.3: Comparison of robust and nominal designs using PSO

	Nominal Design Values	Robust Design Values Cost Considered
Width of Columns (X)	15 inches	19 inches
Depth of Columns (Y)	15 inches	24 inches
Floor Plan Dimensions (L and W)	20 ft by 20 ft	30 ft by 13ft
Area of Bracing in x plane (A_x)	4 in^2	2.60 in^2
Area of Bracing in y plane (A_y)	4 in^2	1.30 in^2
Height of Beams (h_b)	24 inches	12 inches
Strength of Concrete (f_c`)	4000	5500
Column reinforcement ratio (ρ)	0.045	0.08
Sensitivity Index	0.450	0.154
Cost of design	457 units	500 units

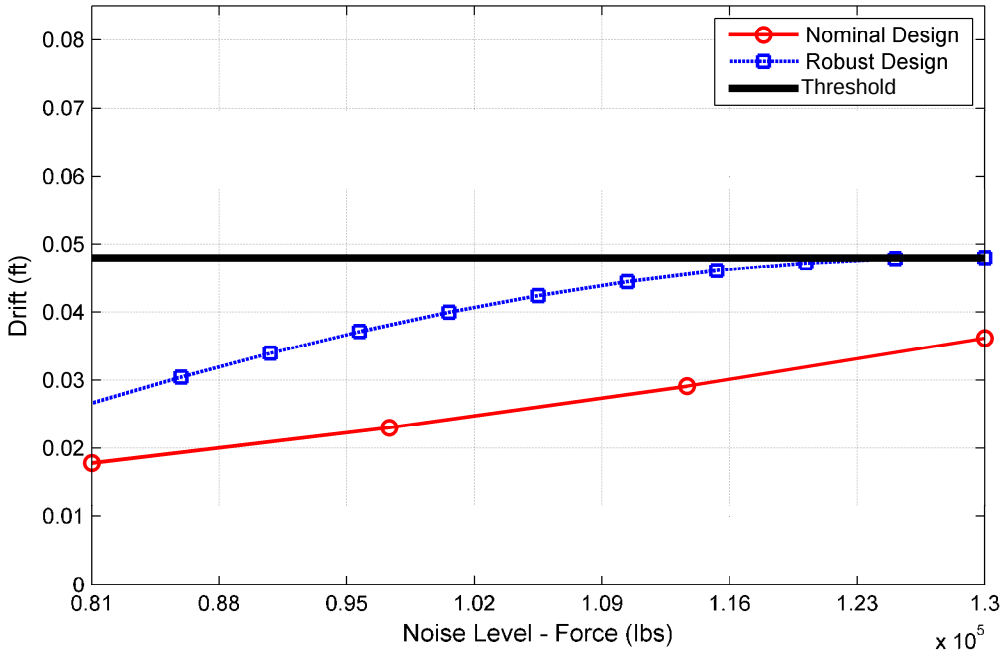

Figure 1.9: Graphical depiction of objective function utilizing particle swarm optimization

6. Conclusion

This chapter presented two methodologies, which successfully demonstrate the application of robust design principles as both a design and a decision making tool for engineers. With the robust optimization methodologies presented here, a single structural design is found which is more insensitive to noise factors than the nominal design, while maintaining, or reducing, the cost for design, thus, proving the misconception that robust designs lead to more expensive, overly designed systems incorrect.

In developing these methodologies, it was discovered that Taguchi's two-step process was not a valid option to use due to the inability to locate a scale factor. Therefore, the decision to develop two single objective optimization methods was necessitated to treat both steps simultaneously; one utilizing the Coordinate Descent Method, and the second utilizing the Particle Swarm Optimization algorithm. Although, these methods were chosen in this study, many more optimization algorithms are available and can be utilized in this work as well.

The Coordinate Descent Method was used to perform a case study to prove the capacity of the proposed methodology in minimizing the objective function and determining a design that satisfies the presented definition of robustness. To provide an illustrative example, a completed iteration of the Coordinate Descent method yielded a design that minimized the Sensitivity Index and decreased cost in comparison to the nominal case.

A more detailed study utilizing the Particle Swarm Optimization method was next completed. Through the use of PSO methods, a more continuous design domain is

established at a computationally tractable manner, allowing the most robust design to be established within the definitions presented in this chapter. The resulting design maximizes its insensitivity to noise factors, while simultaneously ensuring the design's cost stays within an efficient region.

Future work to improve the methods presented in this chapter include work devoted to improving the Sensitivity Index, so that insensitivity and cost are weighed more heavily than proximity to the target threshold. One method for doing so is though a multi-objective optimization study. Also, a probabilistic analysis to formulate real world forces exerted on the structure in a worst case scenario can be explored, concurrent with the introduction of multiple noise sources to the system. This includes examining the importance of applying non-uniformly distributive force distributions. For example, in this study, because a uniform distribution is assumed for the noise factor, the maximum force in the specified range is just as likely to occur as any other force in the range. However, the results can be improved by accepting a more realistic distribution.

This nascent methodology has the potential for practical application in structural design in that the presented robust design methodology is amenable to seek for robustness to extreme events (e.g. earthquakes, hurricanes, blast loading, etc.) and therefore, is a step towards designing for resiliency. Future work should be undertaken to minimize the computational demands for placement in a framework practicing engineers can easily follow.

7. References

[1] Bulleit, William M., “Uncertainty in Structural Engineering,” *Practice Periodical on Structural Design and Construction,* Vol. 13, No. 1, 2008, pp. 24-30.

[2] Mohsine, A., Kharmanda, G., and El-Hami, A., "Improved hybrid method as a robust tool for reliability-based design optimization,." *Structural and Multidisciplinary Optimization,* Vol 32, No. 3, 2006, pp. 203-13.

[3] Wang, Wei, Wu, Justin (Y.-T.) and Lust, Robert V.,“Deterministic Design, Reliability Based Design and Robust Design,“ *Project Report,* Southwest Research Institute and General Motors Research and Development Center.

[4] Chen. W., Wiecek, M., and Zhang, J., "Quality Utility: A Compromise Programming Approach to Robust Design", *ASME Journal of Mechanical Design*, Vol. 121, No. 2, 1999,pp.179-187.

[5] Chen, W., Allen, J.K., Tsui, K-L, and Mistree, F., "A Procedure for Robust Design," *ASME Journal of Mechanical Design*, Vol. 118, No. 4, 1996, 478-485.

[6] Shoemaker, A.C., Tsui, K.-L., & Wu, C.F.J., “Economical Experimentation Methods for Robust Design,” *Technometrics*, Vol. 33, No.4, 1991, pp. 415-427.

[7] Taguchi, G., *Introduction to Quality Engineering: Designing Quality into Products and Processes,* Quality Resources, White Plains, NY, 1986.

[8] Nair, V. N., Abraham, B., MacKay, J., Nelder, J. A., Box, G., Phadke, M. S., et al., “Taguchi's Parameter Design: A Panel Discussion,” *Technometrics*, Vol.34, No.2, 1992, pp. 127-161.

[9] Vanik, M.W., Beck, J.L., and Au, S.K. (2000), "Bayesian Probabilistic Approach to Structural Health Monitoring," *Journal of Engineering Mechanics*, Vol.126, No.7, pp. 738-745.

[10] Beyer, H. and Sendhoff, B., "Robust Optimization – A Comprehensive Survey," *Computer Methods in Applied Mechanics and Engineering*, Vol. 196, 2007, pp. 3190-3218.

[11] Park, Gyung-Jin, Lee, Tae-Hee, Lee, Kwon Hee, and Hwang, Kwang-Hyeon, "Robust Design: An Overview," *AIAA Journal*, Vol. 44, No. 1, 2006, pp. 181-191.

Box, G.E.P., "Signal-to-Noise Ratios, Performance Criteria, and Transformation (with discussion)," *Technometrics*, Vol. 30, No. 1, 1988, pp.1-17.

[12] Phadke, M.S., *Quality Engineering Using Robust Design*, Prentice Hall, Englewood Cliffs, NJ, 1989.

[13] Taguchi, G., *Systems of Experimental Design*, Vols. 1 and 2, Krauss International, New York, 1987.

[14] Cunha, M.d.C., and Sousa, J.J.d.O., "Robust Design of Water Distribution Networks for a Proactive Risk Management," *Journal of Water Resources Planning and Management*, March/April, 2010, pp. 227-236.

[15] Marano, G. C., Sgobba, S., Greco, R., and Mezzina, M., "Robust Optimum Design of Tuned Mass Dampers Devices in Random Vibrations Mitigation," *Journal of Sound and Vibration*, Vol.313, No.3-5, 2008, pp. 472-492.

[16] Unal, R., Wu, K.C., & Stanley, D.O., “Structural Design Optimization for a Space Truss Platform Using Response Surface Methods,” *Quality Engineering*, Vol.9, No.3, 1997, pp. 441-447.

[17] Lee, M.C.W., Mikulik, Z., Kelly, D.W., Thomson, R.S., and Degenhardt, R., “Robust Design- A Concept for Imperfection Insensitive Composite Structures,” *Composite Structures*, No. 92, 2010, pp. 1469-1477.

[18] Schoen, M.P., Hoover, R.C., Chinvorarat, S., and Schoen, G.M., “System Identification and Robust Controller Design Using Genetic Algorithms for Flexible Space Structures,” *Journal of Dynamic Systems, Measurement, and Control*, Vol. 131, 2009.

[19] Kim, J.H., Lee, J.E., and Chang, S.H., “Robust Design of Microfactory Elements with High Stiffness and High Damping Characteristics Using Foam-Composite Sandwich Structures,” *Composite Structures,* No.86, 2008, pp. 220 - 226.

[20] Dehnad, K., *Quality Control, Robust Design, and the Taguchi Method*, Wadsworth and Brooks/Cole, Pacific Grove, CA, 1989.

[21] Ku, K.J., Rao, S.S., and Chen, L., “Taguchi-Aided Search Method for Design Optimization of Engineering Systems,” *Engineering Optimization*, Vol. 30, No. 1, 1998, pp. 1-23.

[22] Box, G.E.P., Bisgaard, S., and Fung, C.A., “An Explanation and Critique of Taguchi’s Contributions to Quality Engineering,” *Quality and Reliability Engineering International*, Vol. 4, No. 2, 1988, pp. 123-131.

[23] Montgomery, D.C., *Design and Analysis of Experiments*, Wiley, Singapore, 1991, pp. 417-433.

[24] Lee, K.H., and Park, G.J., “Robust Design for Unconstrained Optimization Problems Using the Taguchi Method,” *AIAA Journal*, Vol. 34, No. 5, 1996, pp. 1059-1063.

[25] Welch, W. J., Yu, T. K., Kang, S. M., and Sacks, J., “Computer Experiments for Quality Control by Parameter Design,” *Journal of Quality Technology*, Vol. 22, No. 1, 1990, pp. 15–22.

[26] Vining, G. G., and Myers, R. H., “Combining Taguchi and Response Surface Philosophies: A Dual Response Approach,” *Journal of Quality Technology*, Vol. 22, No. 1, 1990, pp. 38–45.

[27] Shoemaker, A. C., and Tsui, K. L., “Response Model Analysis for Robust Design Experiments,” *Communications in Statistics, Part B*, Vol. 22, No. 4, 1993, pp. 1037–1064.

[28] Shiau, G. H., “A Study on the Sintering Properties of Iron Ores Using the Taguchi’s Parameter Design,” *Journal of the Chinese Statistical Association*, Vol. 28, 1990, pp. 253–275.

[29] Tai, C.Y., Chen,T. S., and Wu,M. C., “An Enhanced Taguchi Method for Optimizing SMT Processes,” *Journal of Electronics Manufacturing*, Vol. 2, No. 3, 1992, pp. 91–100.

[30] Tsui, K.-L., “Robust Design Optimization for Multiple Characteristic Problems,” *International Journal of Production Research*, Vol. 37, No. 2, 1999, pp. 433–445.

[31] Rackwitz, R., and Christensen, P. T., *Reliability and Optimization of Structural Systems*, Springer Verlag, 1992.

[32] Rao, S. S., *Engineering Optimization*, Wiley, New York, 1996.

[33] Siddall, J. H., “A New Approach to Probability in Engineering Design and Optimization,” *Journal of Mechanisms, Transmissions, and Automationin Design*, Vol. 106, No. 1, 1984, pp. 5–10.

[34] Chen, X., Sim, M., and Sun, P., “A Robust Optimization Perspective on Stochastic Programming,” *Operations Research,* Vol. 55, No. 66, 2007, pp. 1058-1071.

[35] Eggert, R. J., and Mayne, R. W., “Probabilistic Optimal Design Using Successive Surrogate Probability Function,” *Journal of Mechanical Design*, Vol. 115, No. 3, 1993, pp. 385–391.

[36] Oishi, Y., “Robust Control and Robust Optimization: A Method for Problems with Nonlinear Uncertainty,” *Journal of the Japan Society for Simulation Technology*, Vol. 26, No. 2, 2007, pp. 95-100.

[37] Deb, K., Pratap, A., Agarwal, S., “A Fast and Elitist Multiobjective Genetic algorithm: NSGA-II,” *IEEE Transactions on Evolutionary Computation*, Vol. 6, No. 2, 2002, pp. 182-197.

[38] Kumar, A., Nair, P.B., Keane, A.J., Shahpar, S., “Robust Design Using Bayesian Monte Carlo,” *International Journal for Numerical Methods in engineering*, Vol. 73, 2008, pp. 1497-1517.

[39] Neal, R.M., *Bayesian Learning for Neural Networks.* Springer, Berlin, 1996.

[40] O’Hagan A., and Kennedy, M., and Oakley, J., “Uncertainty Analysis and Other Inference Tools for Complex Compute Codes (with discussion),” *Bayesian Statistics*, Vol. 6, 1999, pp. 503-524.

[41] Construction Publishers and Consultants, *RS Means and Masonry Cost Data 23rd Edition*, Reed Construction Data, Inc., MA, 2005.

[42] ANSYS, Inc., *Theory Reference for ANSYS and ANSYS Workbench*, 2004.

[43] William, K.J. and Warnke, E.D., "Constitutive Model for the Triaxial Behaviour of Concrete," *Proceedings of the International Association for Bridge and Structural Engineering*, Vol. 19, pp.174, ISMES, Bergamo, Italy, 1975.

[44] Z.Q. Luo and P. Tseng (1992), "On the convergence of the coordinate descent method for convex differentiable minimization," *Journal of Optimization Theory and Applications*, Vol. 72, No. 1, pp. 7–35.

[45] J. Nocedal and J. Wright Stephen, Numerical optimization, (2nd ed.), Springer Science & Business Media, NewYork, 2006.

[46] Yingying Li and Stanley Osher, Coordinate descent optimization for l1 minimization with application to compressed sensing: a greedy algorithm. Inverse Problems Imaging, 3 3, 2009, pp. 487–503.

[47] Moore, R., Weldon L., "Interval Analysis and Fuzzy Set Theory," *Fuzzy Sets and Systems*, Vol. 135, No. 1, 2003, pp. 5-9.

[48] Eberhart, R.C., & Kennedy, J., "A New Optimizer Using Particle Swarm Theory," Proceedings of the Sixth International Symposium on Micro Machine and Human Science, IEEE, Nagoya, Japan, 1995, pp. 39-43.

[49] Parsopoulos, K.E., and Vrahatis, M.N., "Parameter Selection and Adaptation in Unified Particle Swarm Optimization," *Mathematical and Computer Modelling*, Vol 46, No. 1-2, 2007, pp. 198-213.

[50] Tsoulos, I.G. and Stavrakoudis, A., "Enhancing PSO Methods for Global Optimization," *Applied Mathematics and Computation*, Vol. 216, No. 10, 2010, pp. 2988-3001.

[51] Plervis, V., and Papadrakakis, M., "A Hybrid Particle Swarm–Gradient Algorithm for Global Structural Optimization," *Computer-Aided Civil and Infrastructure Engineering*, Vol. 26, No. 1, 2011, pp. 48-68.

[52] Eberhart, R.C. and Shi, Y., "Particle Swarm Optimization Developments, Applications and Resources," Proceedings of the International Congress of Evolutionary Computation 2001, IEEE, Vol. 1, 2001, pp. 81-86.

.CHAPTER THREE

STRUCTURAL HEALTH MONITORING FOR SUSTAINABLE AND RESILIENT INFRASTRUCTURE MANAGEMENT

1.0 Introduction

Civil infrastructure ages and deteriorates due to degradation of materials, environmental and location specific issues, overloading and operational factors, and inadequate maintenance and inspection schemes. Deteriorating infrastructure is a worldwide problem, particularly in the United States where a significant portion of the civil infrastructure is approaching, or has passed, its original design lifespan [1]. The American Society of Civil Engineers (ASCE) conducts an infrastructure assessment every two to four years and creates a report card for the nation's infrastructure systems. Since 1998, ASCE has categorized the condition of the nation's civil infrastructure as critical with a grade of D [2,3]. In 2009, ASCE estimated that $2.2 trillion is needed over a five-year period to bring the nation's infrastructure to a good condition [3]. The need to upgrade the nation's aging and deteriorating civil infrastructure with constrained budgets poses a great challenge to infrastructure managers. Thus, it is not only essential to retrofit and reconstruct the existing deteriorating infrastructure systems, but to do so through the use of sustainable infrastructure practices, the purpose of which is to seek maintenance and inspection alternatives that minimize the economic and social costs while maximizing the operational life span of such systems. In order to bring the infrastructure to this condition, major measures must be taken and society's views on how to manage

and maintain infrastructure will need to change. A paradigm shift towards proactive and sustainable infrastructure management schemes is needed. One approach is to equip infrastructure managers with science-based techniques, rather than current qualitative guidelines, for monitoring and assessing the nation's infrastructure.

Current inspection practices rely heavily on expert judgment through visual metrics [4]. Infrastructure systems such as bridges and buildings are assessed based on qualitative guidelines measured against the healthy state of the system [5,6,7]. There is no efficient way of comparing current structural states of the system to the healthy structural state, however. Often because multiple inspectors conduct assessments over the whole lifespan of a structure, a consistent condition baseline is not established over the structure's whole lifespan. The subjective nature of these guidelines can yield vastly different outcomes when completed by different engineers. Moreover, there is an apparent lack of correlation between visual appearance and structural reliability for safety. Thus, metrics and rubrics have been developed by various government and private sector organizations in an attempt to normalize outcomes by providing key elements and condition ratings inspectors should utilize when performing inspections. Tables 2.1 and 2.2 show two different inspection metrics for buildings and bridges, respectively [7,8]. It is essential to equip infrastructure managers with effective quantitative, science-based techniques, rather than qualitative guidelines for monitoring and assessing the ***true*** condition of the nation's infrastructure.

Table 2.1: National Bridge Inspection Standards condition ratings (courtesy of US-DOT, printed with permission).

Code	Description	
N	**Not Applicable**	-
9	**Excellent Condition**	-
8	**Very Good Condition**	No problems noted
7	**Good Condition**	Some minor problems
6	**Satisfactory Condition**	Structural elements show some minor deterioration
5	**Fair Condition**	All primary structural elements are sound but may have some minor section loss from corrosion, cracking, spalling, or scour
4	**Poor Condition**	Advanced section loss, deterioration, spalling, or scour
3	**Serious Condition**	Loss of section, deterioration, spalling, or scour have seriously affected primary structural components. Local failures are possible. Fatigue cracks in steel or shear cracks in concrete may be present.
2	**Critical Condition**	Advanced deterioration of primary structural elements. Fatigue cracks in steel or shear cracks in concrete may be present or scour may have removed substructure support. Unless closely monitored it may be necessary to close the bridge until corrective action is taken.
1	**"Imminent" Failure Condition**	Major deterioration or section loss present in critical structural components or obvious vertical or horizontal movement affecting structure stability. Bridge is closed to traffic but corrective action may put back in light service.
0	**Failed Condition**	Out of service - beyond corrective action.

Table 2.2: Post-disaster building inspection metric. (Courtesy of ATC -20, printed with permission).

	Minor/None	Moderate	Severe	Comments
Overall Hazards:				
Collapse or partial collapse	☐	☐	☐	_____
Building or story leaning	☐	☐	☐	_____
Other _____	☐	☐	☐	_____
Structural Hazards:				
Foundations	☐	☐	☐	_____
Roofs, floors (vertical loads)	☐	☐	☐	_____
Columns, pilasters, corbels	☐	☐	☐	_____
Diaphragms, horizontal bracing	☐	☐	☐	_____
Precast connections	☐	☐	☐	_____
Other _____	☐	☐	☐	_____

Structural Health Monitoring (SHM) is one type of monitoring system useful in diagnosis of structural damage [9]. These monitoring tools, if integrated into a structural system during construction, can gather real-time *in situ* measurements of an infrastructure's performance over its entire life and reduce maintenance costs by locating structural damage before it becomes debilitating [10]. SHM also brings a quantitative metric that, when used properly, can compare current and healthy states to determine the extent of degradation and damage and, moreover, can be applied to predict the lifespan of structural systems. This tool can be used to measure the steady decline in structural functionality, or condition, due to the degrading effects of age and environmental conditions, as well as the severity of damage induced after a disastrous event such as an earthquake, blast, or hurricane. With the ability to quantitatively compare health states, infrastructure managers can easily assess when maintenance is needed, and in the event of a disaster, relay information to emergency managers on severely affected geographical locations needing immediate attention and help.

This research serves as a proof-of concept study for the application of long-term monitoring of infrastructure systems to not only gather information on the structural functionality of the system over time, but also how sustainable or resilient the structural system is as it ages, degrades, and/or becomes damaged. This research focuses on the structural sustainability; however, this approach can be easily applied similarly to the resiliency problem. This can be completed through the development of a novel decision making tool called *Structural Life Cycle Analysis (S-LCA)* charts. In Section Two of this chapter, background concepts, which apply to the conceptual proof of this research will

be explained, followed by a description of the methodology of S-LCA charts and the models employed in conducting this research in Section Three. Section Four presents the results gained from the completion of the study. Finally, Section Five of this chapter will overview the main findings of this study and discuss lessons learned and plans for future work.

2.0 Background

The following section establishes a theoretical framework for the research presented in this chapter. It is categorized into the two distinct topics this research is rooted in: (1) Structural Health Monitoring and (2) Life Cycle Analysis.

2.1 Structural Health Monitoring

Structural Health Monitoring (SHM) is the process of observing a structural system over time using periodically spaced measurements in an effort to compare measured data to *a priori* data of a system in order to gather information on the condition of a system and detect damage [11]. In this context, damage is defined as changes introduced into a system, which adversely affect the functionality of said system, either currently or in the future. General damage types include changes in geometry, material properties, or support conditions, such as alterations in boundary conditions or a reduction in elastic modulus due to cracking or corrosion [9,12,13]. The ability to detect damage and to prescribe appropriate rehabilitation schemes motivates system managers to utilize SHM. Maintenance and repair costs decrease by employing this long-term

monitoring technique, while life-safety impacts are increased. Detecting damage early on reduces the necessity for redundancies, reduces system down-time due to debilitating damage, and alerts officials when systems are unsafe for operation.

The basic concept employed in SHM principles is the dependency of system responses, or *features*, of a structure to its inherent physical properties and characteristics such as mass, stiffness, and damping. As damage occurs and accumulates, these characteristics are altered as is evident through changes in measured responses of the system. Damage detection, as applied in this research, is possible through the comparison of two system states using supervised learning, where data is available for both a damaged and an undamaged system to measure accumulated damage from a base line healthy state [9,12]. For long-term SHM, features are periodically extracted and updated to quantify the ability of a structural system to continue to perform its intended function despite unavoidable aging and damage accumulation resulting from operations and environmental exposure.

SHM methods to quantify damage are especially useful in Civil Engineering applications where damage can occur in places that are not accessible in typical maintenance and inspection routines. Concrete in particular, can exhibit fatal internal cracks and rebar corrosion that can go unseen in current visible inspection schemes. SHM has the capability to detect internal flaws and even predict how much useful life remains in a structural system. This is advantageous for infrastructure managers by allowing them to retrofit damaged structural systems before there is external evidence of damage, an indispensable feature for the development of proactive and sustainable

maintenance and inspection schemes. Several monitoring campaigns utilizing physics-based features, such as strain, displacement, or acceleration have been successfully completed [14-19]; however, none have extended monitoring techniques into an infrastructure management framework to develop science-based metrics to both quantify the health and the sustainability and resiliency of a system over its entire life-span.

2.2 Life Cycle Analysis of Environmental Engineering

The Life Cycle Analysis (LCA), as understood in Environmental Engineering, is a cradle–to-grave investigation and evaluation of the environmental, social, and economic impacts of a given product during the production, use, and disposal phases of its life [20]. LCA follows a product from the collection and extraction of raw materials from the earth to the point where all parts are disposed and returned to the earth [21,22]. The purpose of LCA is to serve as a decision making tool by showing the environmental and social tradeoffs between alternative designs or alterations in a product or system in an effort to improve sustainability. Thus, decision makers may choose the least environmentally, economically, and socially burdensome of available options [23].

LCA tools are quite effective in investigating the impacts caused by a product's existence on a materials, energy, and emissions scale utilizing current LCA frameworks, such as that provided by the US Environmental Protection Agency (LCA 101) [20] or the International Organization for Standardization (ISO 14040) [24]. Although the LCA framework was originally developed to study the rapid depletion of fossil fuels and the concurrent changes in global climate, much research has been conducted on the life cycle

of building products, especially in the resource extraction, manufacturing, and construction phases. Several organizations and agencies have created computer software for this comparative analysis tool which include the National Institute of Standards and Technology's Building for Environmental and Economic Sustainability (BEES), capable of completing life-cycle assessments of over 230 building products [25], the Athena Institute's LCA Model, capable of completing a LCA of *whole* buildings as well as assemblies for new buildings and renovations [26], and Carnegie Mellon University's Economic Input-Output LCA (EIO-LCA), able to estimate the materials and energy resources required, as well as emissions produced for daily activities in an economy [27]. There is currently no tool available, however, that can scientifically measure the structural sustainability of a system over its entire *operational life*, in regards to its measured versus designed performance, rather than on an energy scale. Design life of structures must be incorporated into current LCA practices for a full analysis of a built system.

3.0 Methodologies and Model

3.1 Structural Life Cycle Assessment Concept

Utilizing principles and theories discussed above, it is hypothesized that science-based monitoring and assessment techniques can be developed to provide objective and quantitative information about not only the sustainability, but also the resiliency of our built systems. Such tools can aid in the development of the most cost-effective, long-term

infrastructure management plans and reduce the footprint impact of infrastructure maintenance on energy and materials. This research proposes the construction of *Structural Life-Cycle Analysis (S-LCA) charts.* The research methodologies and results presented herein aim to provide a framework for the development of such a metric by modifying the existing concepts of LCA to provide a holistic, novel, and quantitative approach for structural assessment based on Structural Health Monitoring techniques.

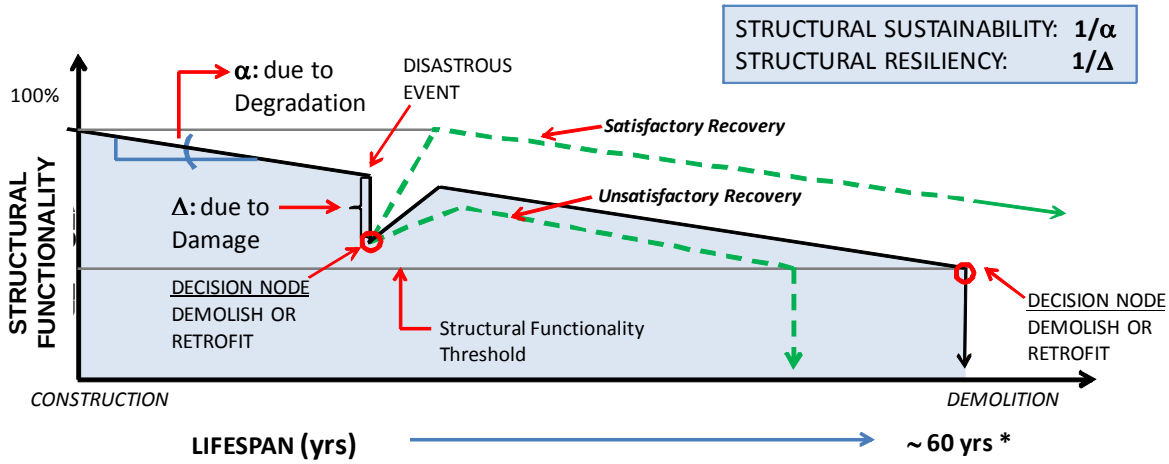

Figure 2.1: SHM can enable us to construct Life-Cycle charts for Structural Sustainability and Resiliency of a structural system.

Figure 2.1 shows a conceptual view of the proposed S-LCA. A built system may be considered 100% structurally functional on the day construction is finished. The degrading effects of aging over the lifespan of a structure will result in a gradual decrease in structural functionality. The rate at which this reduction occurs depends upon the structural sustainability of the built system (1/α in Figure 2.1). During disastrous events, the built system experiences structural damage, the effects of which are evident in the life-cycle chart as an immediate drop of the structural functionality curve. The level at which this reduction occurs depends upon the structural resiliency of the built system

($1/\Delta$ in Figure 2.1). It should be noted that in the context of this research, structural sustainability is a measure of the *degradation* rate, whereas structural resiliency is a measure of the resistance to *damage.* For given environmental and operational conditions, a sustainable and resilient infrastructure would maximize the area under the curve in Figure 2.1.

In SHM, structural degradation and damage are defined as changes that adversely affect the future performance of a built system [13]. Therefore, implicit in the definitions of structural degradation and damage are comparisons against a "reference" system, which often represents the built system in its initial, undamaged condition. We can consider the day the construction is completed as 100% structurally functional, which is the *reference point* for new construction. For an existing structure, however, a reference point for structural functionality must be determined according to the current structural condition. In our formulation, SHM will monitor the deviations of the structure's response from these reference points. The structural degradation and damage accumulation will result in changes in the material and/or geometric properties of the structure. Throughout the lifetime of a built system, the stiffness, mass, or energy dissipation of the structure will be altered, which in turn will result in a measurable change in its system responses. This method can alert infrastructure managers when the functionality drops below a certain level, or if the degradation rate becomes too high.

Using health indices a numerical value for a chosen feature, or features, can be transformed into a structural functionality percentage. To do so, mathematically convenient features are desirable, which are not hidden under large measurement or post-

processing errors. For example, a feature that requires double integration is not preferred because significant numerical errors can propagate into the double integration calculations and possibly produce false positives, a damaged system identification on a truly healthy system, or false negatives, a more serious error in that a truly damaged system is identified to be healthy. The feature should remain valid over the entire serviceable life of the system (i.e. features that become void if nonlinearities develop due to cracking is then useless for the long-term health monitoring of a concrete structure). Lastly, the feature must provide a rational transformation to global condition or health [28]. A successful implementation of SHM can be established through the utilization of the feature qualities discussed above.

3.2 Prototype Structure

For this simulation based proof-of-concept study, a two-story, two-bay, reinforced concrete frame structure was chosen as the prototype. The geometry of the structure is illustrated in Figure 2.2. A structural design for the frame was completed in accordance to ACI 318-08: Building Code Requirements for Structural Concrete and Commentary Standard, 2008 version [29]. The columns are assumed to be fixed to the ground and an idealized operational static wind load was applied to the structure as seen in Figure 2.3, where P is defined as 16 psf.

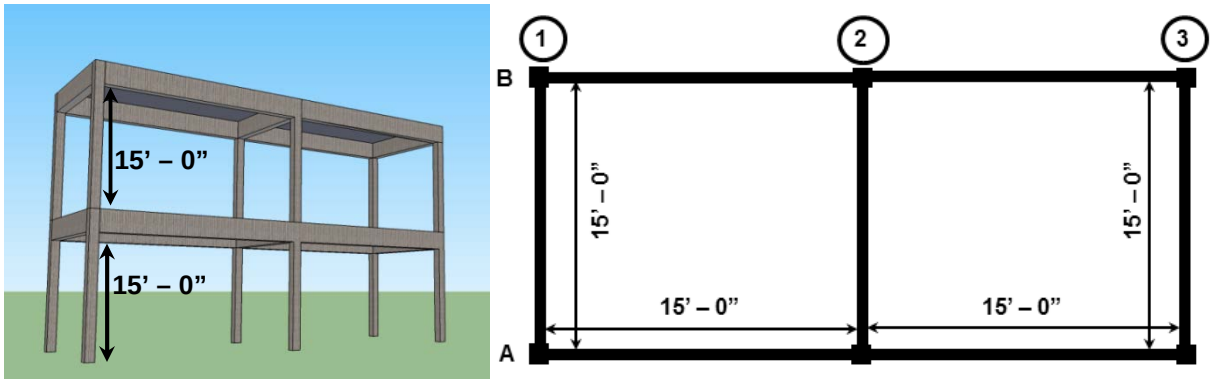

Figure 2.2: Prototype geometry – (a) elevation view (b) plan view

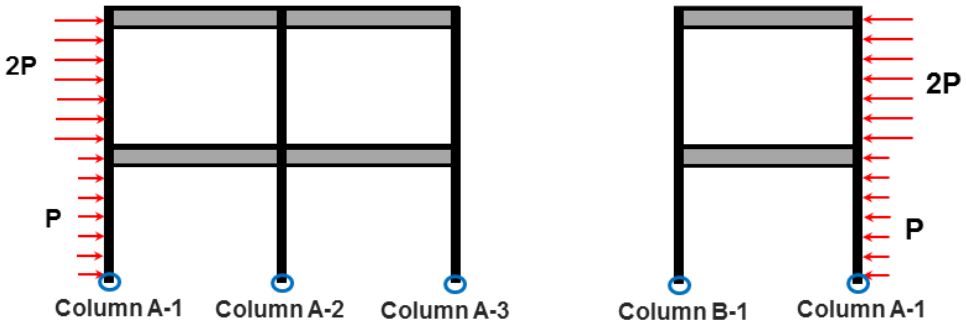

Figure 2.3: Prototype loading

3.3 Finite Element Formulation

Toward the goals outlined in this study, a numerical model of the prototype structure, described in Section 3.2 of this chapter, was developed using the commercial FE modeling package, ANSYS version 13.0. To simulate the complex nonlinear behavior of concrete, Solid65, a solid isoparametric element, is utilized. This particular element is a three-dimensional brick element with eight nodes, each allowing three

translational degrees of freedom in the global x, y, and z directions [30]. As seen in Figure 2.2.4, a multilinear constitutive material model based on the triaxial behavior of concrete developed by William and Warnke was used to define the nonlinear material model in the simulation of failure [31]. With the use of Solid65, the concrete is capable of cracking in three orthogonal directions, plastic deformation, and creep; however, in order to achieve convergence, crushing capabilities were turned off. This element was of particular interest due to the ability to incorporate reinforcement bars directly into the element through by assuming a smeared cross-section, thereby increasing the computational efficiency of the simulation. Although smeared, the rebar modeled in Solid65 is still capable of tension, compression, plastic deformation, and creep.

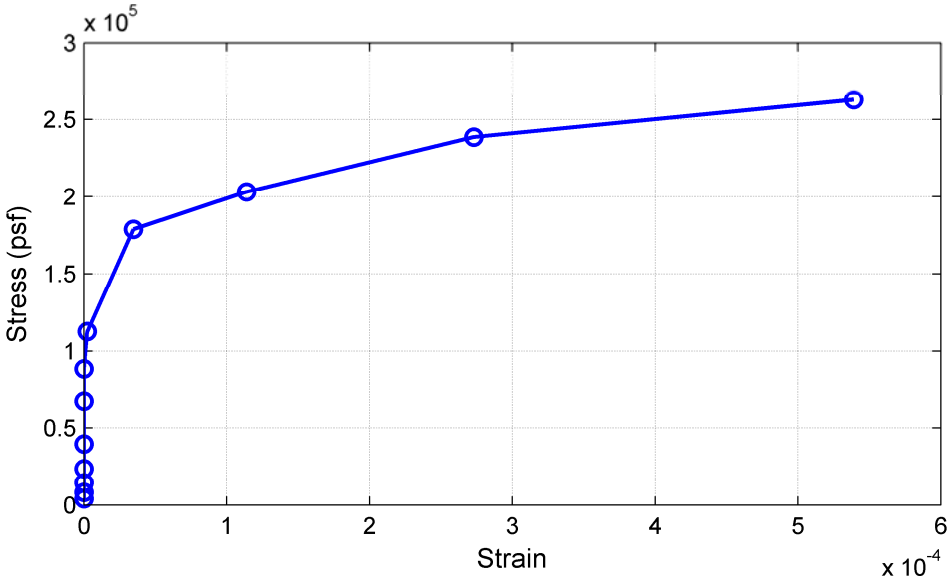

Figure 2.4: Concrete material model

3.4 Degradation Mechanisms

Concrete degradation models are developed to simulate the decrease in structural integrity over a 50 year operational structural lifespan. Herein, the concrete frame is assumed to be located in a marine environment with an average humidity of 70%. With this assumption, it can, with good confidence, also be assumed that corrosion in the concrete frame is inevitable. Therefore, this research will simulate the degrading effects of corrosion while simultaneously modeling the loss of strength due to cracking and general aging.

Steel corrosion is one of the predominant mechanisms of degradation in reinforced concrete structures, the driving forces of which are both complex and widely studied [32,33,34]. The most commonly accepted corrosion model was developed by Tuutti [35] and depicted in Figure 2.5. Known as a bi-linear damage model, the corrosion process is idealized into two-steps [36,37]. The first is an initiation stage, where harmful chlorides penetrate through the solid concrete, eventually reaching the rebar with enough force to initiate corrosion. Here, negligible steel is lost, however, once initiation is reached, the propagation step starts, where significant levels of damage are attained [38]. It has been proven experimentally that the initiation period for offshore

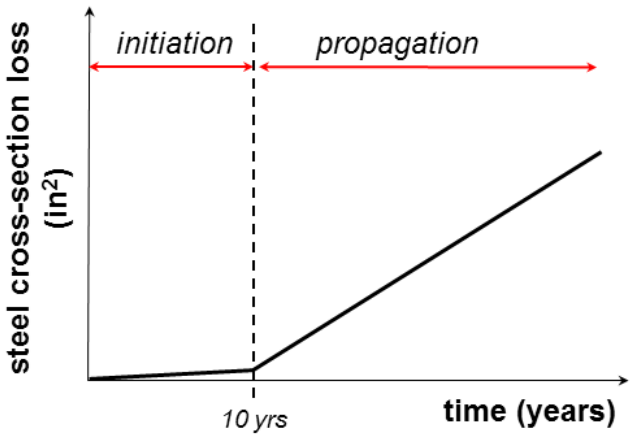

Figure 2.5: Corrosion degradation trends over time ([35])

structures can last ten years, at which point the propagation phase begins and corrosion accumulates [39]. One method of modeling the propagation of corrosion is through the loss of cross-sectional area in the rebar from pitting and rust development. In a single study monitoring the corrosion process of a concrete beam over a 17 year period, researchers found an average loss of two percent of the beam's rebar per year from corrosion after exposure to a chloride rich environment [40]. Thus, this study assumes an initiation period of 10 years and a subsequent two percent reduction in total cross-sectional area per year of operation.

When concrete degrades, it not only corrodes, but also simultaneously loses strength from cracking caused by tensile pressures induced by corrosion, fatigue loading, shrinkage and expansion due to large changes in temperature, and dissolution in material properties due to aging [32-34]. This deterioration in the solid concrete can be captured through an equivalent elastic modulus ($\bar{E}$) which is found by scaling the healthy design elastic modulus (E) by a damage variable (d) as seen in Figure 6a and expressed in Equation 2.1 [41].

$$\bar{E} = (1 - d)\, E \tag{2.1}$$

The damage variable is a function bounded by $0 > d > 1$, where a zero value of d represents a healthy structure and a value of one is an unreachable value without complete failure. This research assumes d is an exponential decay function with a mean lifetime of 0.5 resulting in the exponential decay function found in Equation 2.2. A graphical schematic of the degradation mechanism is provided in Figure 2.6a.

$$d = e^{-2t} \mid 0 < t < 1 \tag{2}$$

Developed in the stress-strain realm, this relationship must be defined over time. Since there is no available model for concrete which specifies the precise amount of degradation per time unit, an exponential relationship between the degradation variable and time is assumed. An example of this relationship is seen below in Figure 2.6b.

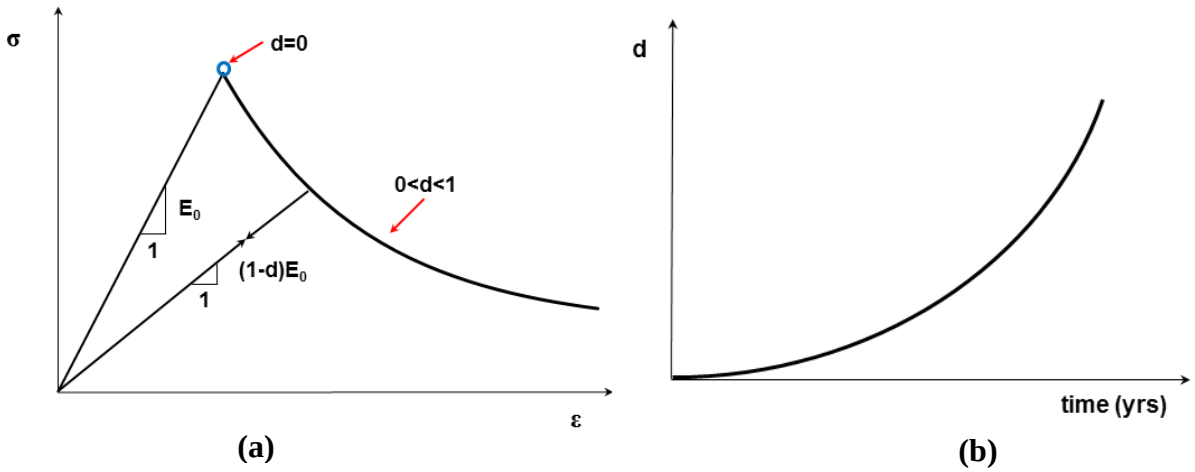

Figure 2.6: Schematics of solid concrete degradation mechanisms – (a) Degradation trend of elastic modulus (b) Relationship of damage variable *d* used in the degradation of the elastic modulus over time.

In this research, the two aforementioned degradation schemes are applied concurrently to the prototype structure discussed in Section 3.2. In that degradation is non-uniform over the entire structure the intent was to study the effect of degradation extent on the Structural Sustainability of a built system and the influence of localization of degradation. The frame is divided into 52 segments as shown in Figure 2.7. Thirty-five segments are then randomly selected for consecutive degradation by corrosive and general degradation forces over a representative 50 years. It should also be noted that exposure to environmental effects is considered when prescribing corrosion levels. If we assume the cross-sectional area of rebar in corner columns degrade at a level of two

percent annually from surface vulnerabilities due to chemical penetration, then beams, columns, and girders with a single exterior face degrade at a rate of 0.75 times over this maximum two percent rate. Similarly, interior beams are specified to degrade at a rate of 0.5 times that of the corner column's two percent. The means used to detect the simulated degradation is discussed in the next section.

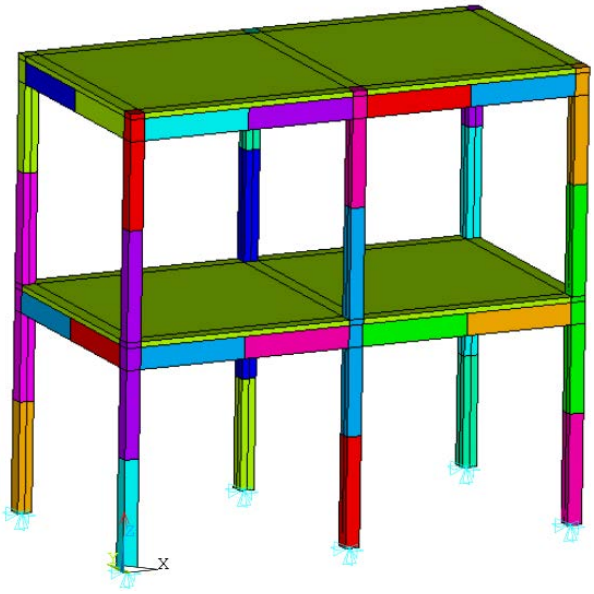

Figure 2.7: Schematic of different degradation locations

3.5 Structural Health Monitoring Campaign

Maximum lateral displacement is a proven method for developing health metrics [28]. In that displacement is inversely related to stiffness, which is affected when cracking or corrosion occurs, the displacements should theoretically increase with a decrease in stiffness properties. This feature, which follows the guidelines for feature selection outlined in Section 3.1, will be used to develop health indices in this study.

The vector sum of displacement will be measured at the roof and first floor levels of each column (Figure 2.2b). Due to the asymmetry of the structure, and subsequent twisting that can occur in deformed shapes caused by damage and degradation, the maximum displacement may change location as the 'effected region' is spatially varied.

Therefore, the maximum lateral displacement on the frame is calculated for each of the 35 degradation scenarios and used in the formulation of S-LCA charts. The SHM process outlined in Figure 2.8 guides the development of health indices. In this process, a negative discrepancy between the damaged structure's response (ω) and the healthy reference point (ω_R) indicates the structure has been degraded or damaged, while a positive discrepancy indicates an improvement in the structural functionality due to repair or recovery campaigns (Figure 2.8). This calculation can then be used to provide the data to alert infrastructure managers of the health of a system.

Figure 2.8: SHM campaign methodology for health monitoring

4.0 Results and Discussion

4.1 Feasibility of SHM Methodology

In the context of this research, a health index is developed ranging from 100% functionality (healthy) to an unattainable value of 0% functionality (failure) by normalizing all data to the displacement value of the healthy structure. Theoretically, the displacement value of the healthy structure should be the smallest measured value unless there is retrofitting which brings the structure's condition to a level which exceeds the

initial *healthy* value. Since the relationship between displacement and health is inversely proportional, i.e. displacement increases with a decrease in health, the normalized values must be inverted to obtain a scale in which the healthy displacement value is a maximum at 100% functionality and the condition is lost as the system degrades or is damaged. When this health index is plotted over the entire lifespan of the structural system, the S-LCA charts proposed in this research materialize.

Figures 2.9 and 2.10 show the ensemble of S-LCA curves achieved after the degradation routine discussed in Section 3.4 is carried out for displacement at the first floor and roof levels, respectively. Each line on the chart represents one degradation segment (i.e. there are 35 lines plotted on each figure). This was completed due to the lack of experimental data in this study. The effect of localized damage was unknown on the global health, thus multiple scenarios were studied. The mean and standard deviations for the distributions are also plotted in ten year increments through the use of error bars, where the square is the mean value and the extending bar represents the even standard deviation. From these figures, it is evident that the metric developed in this research is a plausible visual health metric that can be employed by infrastructure mangers. The health decreases from a 100% functional structure and is detectable in the small localized, segmental degradation scheme utilized in this structure. It should be noted that if there was widespread degradation, such as uniform degradation, the metric proposed here would be able to detect a more drastic decrease in structural integrity.

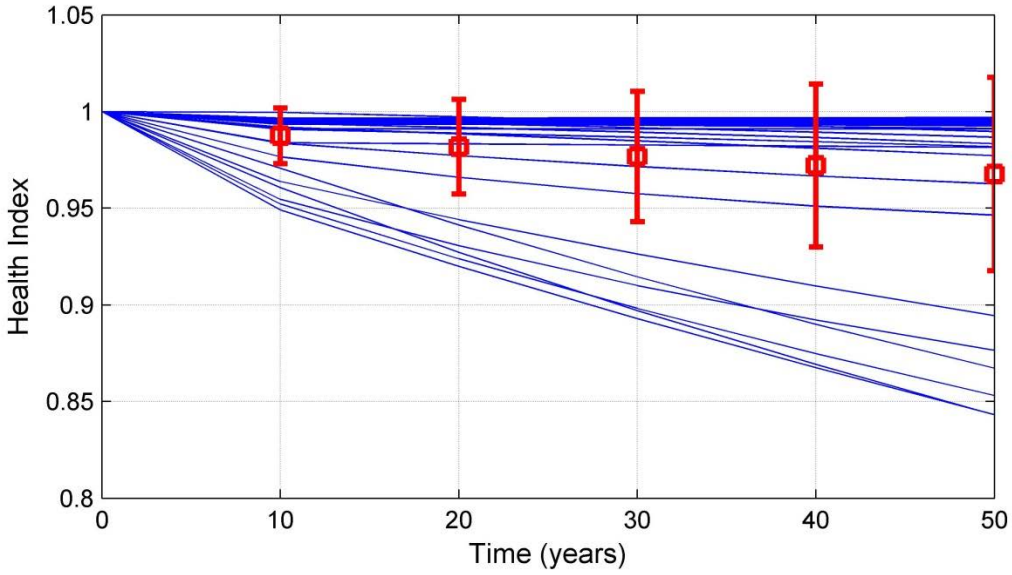

Figure 2.9: Ensemble of degradation S-LCA curves at first floor level

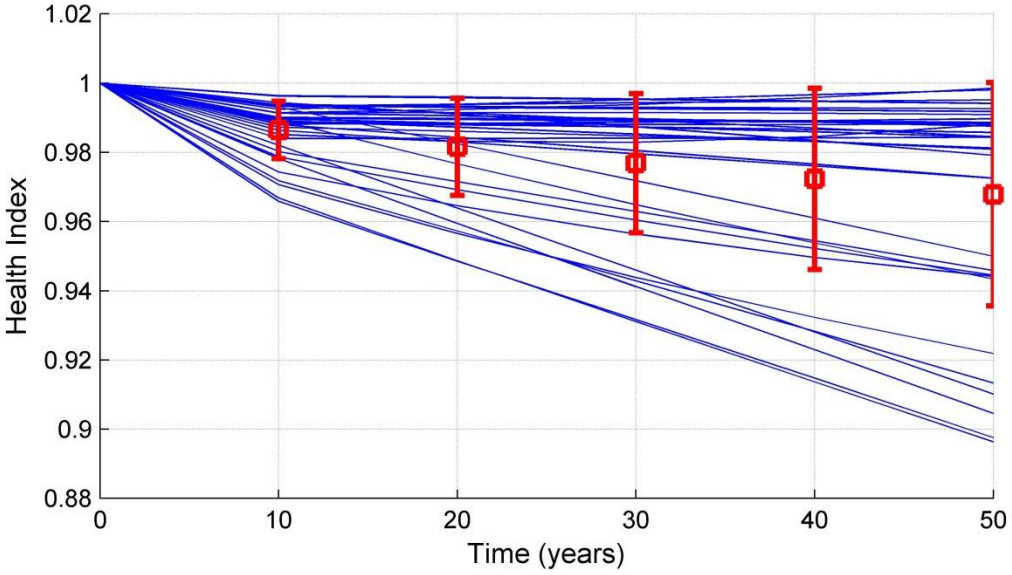

Figure 2.10: Ensemble of degradation S-LCA curves at roof level

The localization of the degradation is imperative when developing maintenance metrics. Certain spatially located degradations are more detectable than others through this approach when exposed to identical degradation rates. Certain locations yield a change in global response as high as 10% (Figure 2.9), while degradation occurring in certain other locations is not as easily detectable, yielding only a 1% change in global system response. Note that when the structure is aging, the degradation will not be fully localized. Therefore, these results should be considered as a worst case scenario. In the next section, the effect of multiple locations degrading simultaneously will be explored.

4.2 Final S-LCA Construction and Sustainability Quantification

The previous section demonstrated a health index that is applicable over a structural system's entire lifespan for localized damage. This section will illustrate and discuss the development of an S-LCA chart and the structural sustainability metric for a more realistic degradation scenario with simultaneous degradation.

As pictured in Figure 2.1 and discussed in Section 3.1, in this chapter, structural sustainability is a measure of the *degradation rate* and inversely relates to the slope of the S-LCA curve. Thus, the structural sustainability will be calculated in ten year increments as defined in Equation 2.3, where SS is structural sustainability, I_i is the inspection interval (number of years between health measurements, 10 in this case), n is the number of health measurements taken (including the healthy measurement), h_{i-1} is the health index value of the previous measurement point, and h_i is the health index value at the current measurement point.

$$SS = \frac{I_i(n-1)}{\sum h_{i-1} - h_i} \tag{2.3}$$

Thusly, infrastructure managers can compare current and past structural sustainability performance. If desired, an average structural sustainability value can be periodically updated as more measurements are taken, and the S-LCA chart develops over time.

To prove the feasibility of this concept for more extensive degradation, the degradation scheme outlined in Table 2.3 is adopted. Segments are sequentially added to the degradation process and the cumulative effect on the structure increases with time. Similar to the single segment degradation case, multiple degradation scenarios were simulated in the absence of experimental data. Figure 2.11 shows an ensemble plot of 20 random degradation scenarios, much like the plot illustrated in Figures 2.10 and 2.11. This figure shows the increase in global degradation with multiple segments simultaneously degraded.

Table 2.3: Degradation scheme for multiple segments degrading simultaneously

Year 10	2 segments @10 yr rate
Year 20	5 segments @ 10 yr rate, 2 segments @ 20 yr rate
Year 30	7 segments @ 10 yr rate, 5 segments @20 yr rate, 2 segments @30 yr rate
Year 40	9 segments @ 10 yr rate, 7 segments @ 20 yr rate, 5 segments @ 30 yr rate, 2 segments @ 40 yr rate
Year 50	12 segments @ 10 yr rate, 9 segments @ 20 yr rate, 7 segments @ 30 yr rate, 5 segments @ 20 yr rate, 2 segments @ 50 yr rate

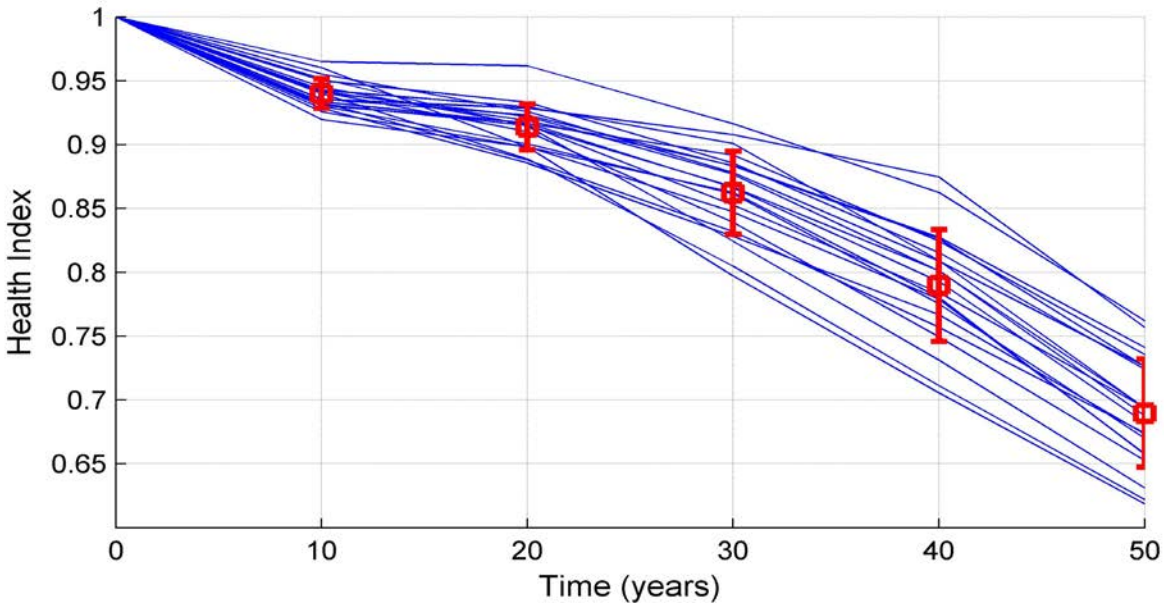

Figure 2.11: Ensemble figure for 20 random degradation scenarios with multiple segments simultaneously degraded

The mean value from data obtained in Figure 2.11 is used to create the final form of the S-LCA chart seen in Figure 2.12. Since this is a simulation and not an experiment with one data set, any of the curves could be taken to construct the final S-LCA chart, the mean was taken for illustrative purposes. It should also be noted that Figure 2.1 idealizes what form S-LCA charts will take. Figure 2.12 shows that the degradation rate is non-constant over the structure's entire life. There will be some years that experience more degradation than others, thus creating segmented S-LCA charts. For this case, since multiple *inspection data* is available, the Structural Sustainability can be calculated (Equation 2.3) in each interval. These values are shown in Table 2.4. The average Structural Sustainability was calculated to be 196.51, a measure of how well the structure's response can resist degradation. Table 2.4 also shows the evolution of this metric as the structure ages and degradation is accumulated. With this metric, the greater

the Structural Sustainability, the more apt you are to maximizing the area under the S-LCA curve, after all with a slope of zero, this metric yields a Structural Sustainability value of infinity. With this in mind, you can see the years where degradation was most severe, mainly the inspection period between years 0 and 10 and between years 40 and 50. This hypothesis is affirmed when compared to the S-LCA chart.

Table 2.4: Structural Sustainability values over time

	Year 0-10	Year 10-20	Year 20-30	Year 30-40	Year 40-50	**Average**
Structural Sustainability	166.39	384.62	193.80	137.93	99.80	**196.51**

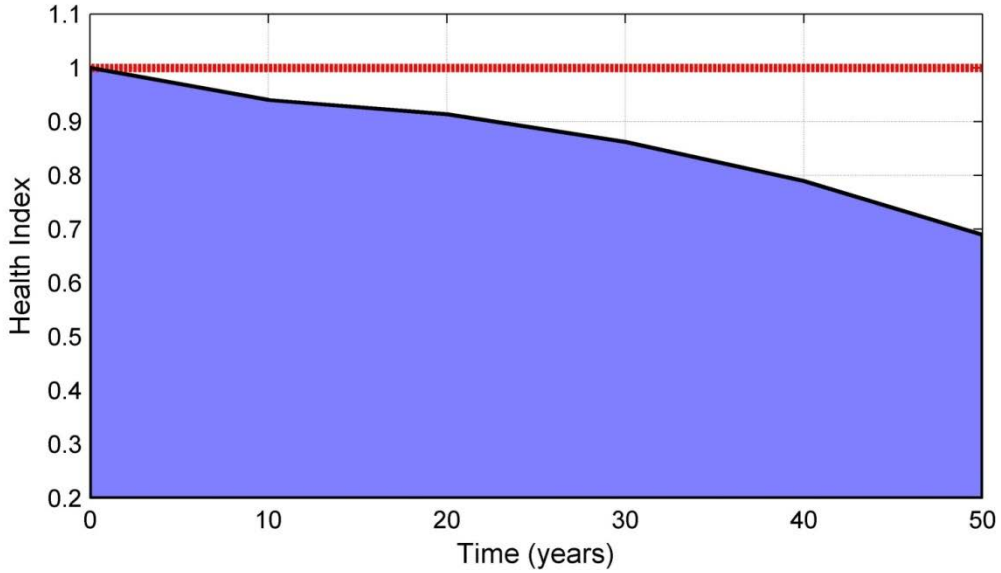

Figure 2.12: S-LCA chart for multiple segments simultaneously degraded over the structure's whole life

This chart is advantageous when measuring past performance, but also for prognostic purposes. Through the establishment of degradation trends, infrastructure managers are able to schedule inspections and predict when maintenance will be necessary.

5.0 Conclusions

With the numerous failing and deficient infrastructure systems in the United States, it has become ever more important to develop indices and metrics to serve as proactive infrastructure management schemes. Both neglect and setbacks due to financial constraints have resulted in such failing infrastructures. To mitigate similar circumstances from occurring again, it is necessary to develop metrics to quantitatively measure the degradation of infrastructures. This will allow rehabilitation to be completed when damage and detectable deterioration *occur*, not when they become debilitating. Such proactive measures, which can save vast capital are proven a sustainable maintenance scheme. By allowing managers to view and quantify a decrease in degradation, they can maximize the area under the S-LCA curve. Thusly, the novel aspect of this research is validated in that it casts sustainability and resiliency in a quantifiable framework where designs can be compared and implemented accordingly.

This research clearly confirms that Structural Life Cycle Assessment (S-LCA) charts are one possible method for quantifying the health and sustainability of an infrastructure system through its entire life cycle via implementation of Structural Health Monitoring practices and Life Cycle Assessment principles. Through this research, the applicability of this method for both minor and more extensive degradation over the entire lifespan of a structural system is proven. Degradation was simulated in the concrete structure through corrosive forces, represented by a loss in cross-sectional area in the steel rebar, and loss of strength, represented through the application of an *effective elastic modulus.* The effects of damage localization on the chosen feature were

discovered when degradation was applied spatially, one segment at a time. The subsequent spread of health indices fell between a 1% loss in global structural condition to an almost 10% loss in global structural condition. To apply a more realistic degradation scheme and to illustrate the development of the sustainability metric, the sequential addition of degraded members was simulated. Through this method, the time dependent accumulation of degradation was captured with a visual decrease in both the health index and the Structural Sustainability metric over time.

Because, this simulation based study encompassed only factors intentionally introduced to affect the system, false diagnostics from ambient factors are possible in operational settings. Future research must improve and expand upon the concepts presented here, and explore the robustness of features used in the construction of S-LCA charts regarding the influences factors that can cause noise and false diagnostics. Accounting for wind fluctuations and changes in temperature and humidity is also necessary before this method can be fully embraced by infrastructure managers. Also, a study in resiliency to extreme factors should be conducted.

6.0 References

[1] Zhu, J., and Popovics, J.S. (2008), “Non-contact NDT of Concrete Structures Using Air Coupled Sensors,” Newark Structural Engineering Laboratory report NSEL-010.

[2] American Society of Civil Engineers (1998), “1998 Report Card for America's Infrastructure.”

[3] American Society of Civil Engineers (2009), “2009 Report Card for America's Infrastructure.”

[4] ASCE/SEI-AASHTO Ad-Hoc Group on Bridge Inspection, Rating, Rehabilitation, and Replacement (2009), “White Paper on Bridge Inspection and Rating,” *Journal of Bridge Engineering,* Vol. 14, No. 1, pp. 1-5.

[5] Stillman, J. (1992), “Design Life and the New Code,” in *The Design Life of Structures,* Ed. Somerville, G., Blackie and Son Ltd, Glasgow, NZ.

[6] Schmaltz, T.C., and Stiemer, S.F. (1995), “Consideration of Design Life of Structures,” *Journal of Performance of Constructed Facilities*, Vol.9, No. 3, pp.206 – 219.

[7] Applied Technology Council (1995), “ATC-20 Set Procedures for Postearthquake Safety Evaluation of Buildings.”

[8] U.S. Department of Transportation. (1995), “Recording and Coding Guide for the Structure Inventory and Appraisal of the Nation’s Bridges,” Federal Highway Administration report FHWY-PD-96-001.

[9] Farrar, C.R., and Worden, K. (2007), "An Introduction to Structural Health Monitoring," *Philosophical Transactions of the Royal Society A*, Vol. 365, pp. 303-315.

[10] Enright, M. P., and Frangopol, D. M. (2000). ‘‘Reliability based lifetime maintenance of aging highway bridges.’’ Proc., SPIE’s 6th Int. Symposium on NDE and Health Monitoring and Diagnostics. Nondestructive Evaluation of Highways, Utilities and Pipelines, A. E. Aktan and S. R. Gosselin, eds., International Society for Optical Engineering, Bellingham, Wash., Vol. 3995, 4–13.

[11] Doebling, S.W., Farrar, C.R., Prime, M.B., and Shevitz, D.W. (1996), “Damage Identification and Health Monitoring of Structural and Mechanical Systems from

Changes in their Vibration Characteristics: A Literature Review," Los Alamos National Laboratory report LA-13070-MS.

[12] Worden, K., Farrar, C.R., Manson, G., amd Park, G. (2007), "The Fundamental Axioms of Structural Health Monitoring," *Proceedings of the Royal Society,* Vol. 463, pp. 1639-1664.

[13] Sohn, H., Farrar, C.R., Hemez, F.M., Shunk, D.D., Stinemates, D.W., and Nadler, B.R. (2004), "A Review of Structural Health Monitoring Literature from 1996-2001," Los Alamos National Laboratory report LA-13976-MS.

[14] Catbas, F.N., Grimmelsman, K.A., and Aktan, A.E. (2000), "Structural Identification of the Commodore Barry Bridge," *Proc. SPIE,* Vol. 3995, pp. 84-97.

[15] Jeary, A.P., Soarks, P.R., and DeSouza, V.C.M. (1981), "A study on the Use of Ambient Vibration Measurements to Detect Changes in the Structural Characteristics of a Building," *Proceedings from ASCE EMD Specialty Conference – Dynamic Response of Structures,* Atlanta, GA, pp. 189-199.

[16] Jeary, A.P., Chui, G.C., and Wong, J.C.K. (2001), "Wholistic Structural Appraisal," *Proceedings from the 8th International Conference and Structural Safety and Reliability: ICOSSAR 200.*

[17] Wenzel, H. and Pichler, D. (2005), *Ambient Vibration Monitoring,* J. Wiley and Sons Ltd., Chichester.

[18] Asmussen, J.C. (1997), *Modal Analysis Based on the Random Decrement Technique – Application to Civil Engineering Structures,* Department of Building Technology and Structural Engineering, University of Aalborg, Denmark.

[19] Brownjohn, J.M. (2007), "Structural Health Monitoring of Civil Infrastructure," *Philosophical Transactions of the Royal Society,* Vol. 365, pp. 589-622.

[20] Environmental Protection Agency. *Scientific Applications International Corporation. Life Cycle Assessment: Principles and Practice*. Rep. no. 68-C02-067. Cincinnati: U.S. Environmental Protection Agency, 2006.

[21] Trusty, W.B. and Horst, S. (2003), "Integrating LCA Tools in Green Building Rating Systems," *The Athena Institute,* available online at www.athenasmi.ca

[22] Kibert, J. (2005), *Sustainable Construction: Green Building Design and Delivery*, John Wiley and Sons, Inc., Hoboken, NJ.

[23] Curran, M. A. (1996), *Environmental Life-Cycle Assessment,* McGraw Hill, New York, NY.

[24] International Organization for Standardization. (2006) *Environmental management -- Life cycle assessment --Principles and framework.* Rep. no. ISO 14040:2006(E). 2nd ed. Switzerland.

[25] Lippiatt, Barbara C. *BEES 4.0: Building for Environmental and Economic Sustainability Technical Manual and User Guide*. Rep. no. NISTIR 7423. Gaithersburg: National Institute of Standards and Technology, 2007.

[26] Athena Institute. (2010). LCA Model. from http://www.athenasmi.org/about/lcaModel.html.

[27] Carnegie Mellon University Green Design Institute (2010). Economic Input-Output Life Cycle Assessment. from http://www.eiolca.net/.

[28] Catbas, F.N. and Aktan, A.E. (2002), "Condition and Damage Assessment: Issues and Some Promising Indices," *Journal of Structural Engineering*, Vol. 128, No. 8, pp. 1026-1036.

[29] American Concrete Institute. (2008), "318-08: Building Code Requirements for Structural Concrete and Commentary."

[30] ANSYS, Inc. (2004), *Theory Reference for ANSYS and ANSYS Workbench.*

[31] William, K.J. and Warnke, E.D. (1975) "Constitutive Model for the Triaxial Behaviour of Concrete," *Proceedings of the International Association for Bridge and Structural Engineering*, Vol. 19, pp.174, ISMES, Bergamo, Italy.

[32] Zhao, Y., Yu, J., Jin, W. (2011) "Damage Analysis and Cracking Model of Reinforced Concrete Structures with Rebar Corrosion," *Corrosion Science*, Vol. 53, No. 10, pp. 3388-3397.

[33] Bhargava, K., Mori, Y., Ghosh, A.K. (2011), "Time-dependent Reliability of Corrosion-affected RC Beams – Part 1: Estimation of Time-dependent Strengths and Associated Variability," *Nuclear Engineering and Design*, Vol. 241, No. 5, pp. 1371-1384.

[34] Zhong, J.Q., Gardoni, P., Rosowsky, D., (2010), "Stiffness Degradation and Time Cracking of Cover Concrete in Reinforced Concrete Structures Subject to Corrosion," *Journal of Engineering Mechanics*, Vol. 136, No. 2, pp. 209-219.

[35]Tuutti, K. (1982) "Corrosion of Steel in Concrete," Research Report No 4, Swedish Cement and Concrete Research Institute, Stickholm, pp. 17-21.

[36] Bertolini, L., Elsener, B., Pedeferri, P., Polder R. (2004), “Corrosion of Steel in Concrete,” Wiley-VCH, Weinheim.

[37] Polder, R.B., de Rooij, M.R. (2005) “Durability of Marine Concrete Structures — Field Investigations and Modelling," *Heron 50,* Vol. 3, pp. 133–153.

[38] Martin-Perez, B. and Lounis, Z. (2003) “Numerical Modelling of Service Life of Reinforced Concrete Structures,” *Proceedings of the 2nd International RILEM Workshop on Life Prediction and Aging Management,* Paris, France, pp. 71-79.

[39] Melchers, R.E. and Li, C.Q. (2009) “Reinforcement Corrosion Initiation and Activation Times in Concrete Structures Exposed to Severe Marine Environments,” *Cement and Concrete Research,* Vol. 39, pp. 1068-1076.

[40] Vidal, T., Castel, A., Francois, R. (2007) “Corrosion Process and Structural Performance of a 17 Year Old Reinforced Concrete Beam Stored in Chloride Environment,” *Cement and Concrete Research,* Vol. 37, No. 11, pp. 1551-1561.

[41] Hanganu, A.D., Oñate, E., Barbat, A.H. (2002) “A Finite Element Methodology for Local/Global Damage Evaluation in Civil Engineering Structures,” *Computers and Structures,* Vol. 80, pp.1667-1687.

CHAPTER FOUR

CONCLUSIONS

Presented in this thesis are the results from two studies that develop novel design and maintenance routines to promote sustainability and resiliency in infrastructure systems. In doing so, this research aims to provide tools that can be used to prolong the lifespan of infrastructure systems, both in the design phase and operational phase.

First, the feasibility of the application of robust design principles to the structural engineering process was examined through the use of two optimization methods – the Coordinate Descent Optimization method and the Particle Swarm Optimization method. Using these methods and the robust design methodologies presented in Chapter 2 of this thesis, a single structural design can be found which is more insensitive to noise factors and maintains, or minimizes the cost compared to some nominal design. Future work to improve the methods and concepts presented in the work chronicled in Chapter 2 of this thesis include the improvement of the Sensitivity Index and completing a probabilistic analysis to impose more realistic noise forces.

Next, the research presented in Chapter 3 of this thesis has shown that Structural Life Cycle Assessment (S-LCA) charts are a plausible and effective way of assessing the health and sustainability of infrastructure systems in order to prolong the life of an infrastructure system. This was proven effective by using Structural Health Monitoring and Life Cycle Assessment principles. This research demonstrates the feasibility of the S-LCA approach for both minor and more extensive damage over the entire lifespan of a structural system. However, since this study was solely simulation based, an operational

application is necessary to fully validate the concept presented here. Further research on the robustness of features to fluctuating environmental factors should be carried out to minimize false diagnostics.

Both concepts presented in this thesis promote sustainability and resiliency in the civil infrastructure realm. Currently, these two concepts were examined separately; however, future work to incorporate these two concepts can produce an interesting and compelling study. Robust designs developed in Chapter Two can be compared to nominal cases to examine the design configuration's robustness to degradation by following the procedure outlined in Chapter Three. The completion of this work has the potential to provide more feasibility in the adaptation of robust design principles to the world of practicing design engineers.

APPENDIX: FE CODE SAMPLE

This appendix provides a sample from the developed FE code utilized in Chapter Two of this thesis. This code is used to automate the process of constructing a concrete frame FE model. With the user supplied values for each of the eight design parameters and noise forces, this code constructs the geometry of the model, specifies material properties and real constants, meshes the geometry and assigns material properties, sets solution controls to assure convergence, applies boundary conditions and loads, and finally solves for displacement at the desired location.

```
RESUME, 'ModelWithBracing','db','.'
/PREP7

xx1 = \\${X}
xx2 = xx1+\\${A}
xx3 = xx1+xx2
xx4 = xx1/2
xx5 = xx1+0.5
xx6 = xx2-0.5
xx7 = xx2+xx4

yy1 = \\${Y}
yy2 = yy1+\\${B}
yy3 = yy1+yy2
yy4 = yy1/2
yy5 = yy1+0.5
yy6 = yy2-0.5
yy7 = yy2+yy4

zz1 = 0.5
zz2 = 1
zz3 = 14.5-\\${Hb}
zz4 = 15-\\${Hb}
zz5 = 15
zz6 = 15.375

Fc = \\${STRGTHCONC}
CRACK = 7.5*SQRT\(Fc\)*144
Epsi = 57000*SQRT\(Fc\)
STRAIN0 = \(2*Fc\)/\(Epsi\)
STRAIN1 = \(0.30*Fc\)/\(Epsi\)
STRESS1 = 0.3*Fc*144
E = Epsi*144
STRESS2 =
\(\(Epsi*0.00078\)/\(1+\(\(0.00078/STRAIN0\)*\(0.00078/STRAIN0\)\
)\)\)*144
STRESS3 =
\(\(Epsi*0.00123\)/\(1+\(\(0.00123/STRAIN0\)*\(0.00123/STRAIN0\)\
)\)\)*144
STRESS4 =
\(\(Epsi*0.00168\)/\(1+\(\(0.00168/STRAIN0\)*\(0.00168/STRAIN0\)\
)\)\)*144
```

```
STRESS5 =
\(\(Epsi*0.0022\)/\(1+\(\(0.0022/STRAIN0\)*\(0.0022/STRAIN0\)\)\)
\)*144

!COLUMN A1
K     ,     1     ,     0     ,     0     ,     0
K     ,     2     ,     xx1   ,     0     ,     0
K     ,     3     ,     xx1   ,     yy1   ,     0
K     ,     4     ,     0     ,     yy1   ,     0
K     ,     5     ,     xx1   ,     yy4   ,     0
K     ,     6     ,     xx4   ,     yy1   ,     0
K     ,     101   ,     0     ,     0     ,     zz1
K     ,     102   ,     xx1   ,     0     ,     zz1
K     ,     103   ,     xx1   ,     yy1   ,     zz1
K     ,     104   ,     0     ,     yy1   ,     zz1
K     ,     105   ,     xx1   ,     yy4   ,     zz1
K     ,     106   ,     xx4   ,     yy1   ,     zz1
K     ,     201   ,     0     ,     0     ,     zz2
K     ,     202   ,     xx1   ,     0     ,     zz2
K     ,     203   ,     xx1   ,     yy1   ,     zz2
K     ,     204   ,     0     ,     yy1   ,     zz2
K     ,     205   ,     xx1   ,     yy4   ,     zz2
K     ,     206   ,     xx4   ,     yy1   ,     zz2
K     ,     301   ,     0     ,     0     ,     zz3
K     ,     302   ,     xx1   ,     0     ,     zz3
K     ,     303   ,     xx1   ,     yy1   ,     zz3
K     ,     304   ,     0     ,     yy1   ,     zz3
K     ,     305   ,     xx1   ,     yy4   ,     zz3
K     ,     306   ,     xx4   ,     yy1   ,     zz3
K     ,     401   ,     0     ,     0     ,     zz4
K     ,     402   ,     xx1   ,     0     ,     zz4
K     ,     403   ,     xx1   ,     yy1   ,     zz4
K     ,     404   ,     0     ,     yy1   ,     zz4
K     ,     405   ,     xx1   ,     yy4   ,     zz4
K     ,     406   ,     xx4   ,     yy1   ,     zz4
K     ,     501   ,     0     ,     0     ,     zz5
K     ,     502   ,     xx1   ,     0     ,     zz5
K     ,     503   ,     xx1   ,     yy1   ,     zz5
K     ,     504   ,     0     ,     yy1   ,     zz5
K     ,     601   ,     0     ,     0     ,     zz6
K     ,     602   ,     xx1   ,     0     ,     zz6
K     ,     603   ,     xx1   ,     yy1   ,     zz6
K           604   ,     0     ,     yy1   ,     zz6


.
.     CONTINUE SPECIFYING KEYPOINTS FOR WHOLE STRUCTURE
.


!CREATE AREAS COLUMN A1    ,

A,    1,    2,    5,    3,    6,    4
A,    2,    5,    105,  205,  305,  405,  402,  302,  202,  102
A,    5,    3,    103,  203,  303,  403,  405,  305,  205,  105
```

```
A,    3,    6,    106,  206,  306,  406,  403,  303,  203,  103
A,    6,    4,    104,  204,  304,  404,  406,  306,  206,  106
A,    4,    1,    101,  201,  301,  401,  404,  304,  204,  104
A,    1,    2,    102,  202,  302,  402,  401,  301,  201,  101
A,    402,  405,  403,  503,  502
A,    403,  406,  404,  504,  503
A,    404,  401,  501,  504
A,    401,  402,  502,  501
A,    502,  503,  603,  602
A,    503,  504,  604,  603
A,    504,  501,  601,  604
A,    501,  502,  602,  601
A,    601,  602,  603,  604

!CREATE VOLUMES COLUMN A1 \(VOLUME 1\)
ASEL,S,AREA,,1,16,1
VA,ALL


.
.     CONTINUE CREATING AREAS AND VOLUMES FOR WHOLE STRUCTURE
.


!CREATE CROSSBRACING
!GIRDER A1-A2 \(LINES 261-278\)
L,302,7
L,402,107
L,425,207
L,305,12
L,405,112
L,427,212
L,303,10
L,403,110
L,429,210
L,307,2
L,407,102
L,426,202
L,312,5
L,412,105
L,428,205
L,310,3
L,410,103
L,430,203
!BEAM A1-B1 \(LINES 279-296\)
L,313,4
L,413,104
L,434,204
L,317,6
L,417,106
L,435,206
L,314,3
L,414,103
L,436,203
```

```
L,304,13
L,404,113
L,431,213
L,306,17
L,406,117
L,432,217
L,303,14
L,403,114
L,433,214


.
.     CONTINUE CREATING CROSS BRACING FOR WHOLE STRUCTURE
.


!SPECIFY MATERIAL MODELS
!SOLID CONCRETE
!MAT1
!ELASTIC MODEL
MPTEMP,,,,,,,,
MPTEMP,1,0
MPDATA,DENS,1,,4.6584
MPTEMP,,,,,,,,
MPTEMP,1,0
MPDATA,EX,1,,E
MPDATA,PRXY,1,,0.2
!CONCRETE MODEL
TB,CONC,1,,,
TBDATA,,0.2,1.0,CRACK,-1,0,0
TBDATA,,0,0,0,,,
!MULTILINEAR ELASTIC
TB,MELA,1,1,6,
TBPT,,0,0
TBPT,,STRAIN1,STRESS1
TBPT,,0.00078,STRESS2
TBPT,,0.00123,STRESS3
TBPT,,0.00168,STRESS4
TBPT,,0.0022,STRESS5

!STEEL REBAR
!MAT2
MPDATA,EX,2,,4176000000
MPDATA,PRXY,2,,0.3
MPDATA,DENS,2,,15.2174

!STEEL CROSSBRACING
!MAT3
MPDATA,EX,3,,4200000000
MPDATA,PRXY,3,,0.3
MPDATA,DENS,3,,15.22

!SPECIFY REAL CONSTANTS
!COLUMNS REAL1
R,1,2,\\${RCOL},0,90, , ,
```

```
RMORE, , , , , , ,
RMORE, ,


.
.     CONTINUE SPECIFYING MATERIAL MODEL AND REAL CONSTANTS
.


!MESH MODEL
!MESH CROSSBRACING Y dir
TYPE,2
MAT,3
REAL,6
ESYS,0
SECNUM,
LSEL,S,,,279,314,1
LESIZE,ALL, , ,1, , , , ,1
LMESH,ALL
ALLSEL,ALL
!MESH CROSSBRACING X dir
TYPE,2
MAT,3
REAL,5
ESYS,0
SECNUM,
LSEL,S,,,261,278,1
LSEL,A,,,315,332,1
LESIZE,ALL, , ,1, , , , ,1
LMESH,ALL
ALLSEL,ALL

!MESH COLUMN A1
TYPE,1
MAT,1
REAL,1
ESYS,0
SECNUM,
LSEL,S,LINE,,13
LSEL,A,LINE,,9
LSEL,A,LINE,,18
LSEL,A,LINE,,23
LSEL,A,LINE,,28
LSEL,A,LINE,,33
LSEL,A,LINE,,39
LSEL,A,LINE,,37
LSEL,A,LINE,,40
LSEL,A,LINE,,42
LSEL,A,LINE,,1,6,1
LSEL,A,LINE,,36
LSEL,A,LINE,,11
LSEL,A,LINE,,20
LSEL,A,LINE,,25
LSEL,A,LINE,,30
```

```
LSEL,A,LINE,,35
LESIZE,ALL,0.25,,,,,,1
ALLSEL,ALL
VSWEEP,1


.
.     CONTINUE MESHING WHOLE GEOMETRY
.


/SOLU

NLGEOM,ON
NSUBST,1,1000,1
OUTRES,ALL,ALL
AUTOTS,ON
CNVTOL,,-1,23
CNVTOL,,-1,24
CNVTOL,U, ,0.25,2, ,
LNSRCH,0
NCNV,2,20,0,0,0
NEQIT,10000

!SPECIFY ANALYSIS TYPE
ANTYPE,0

!FIX COLUMNS AT BASE
DA,1,ALL,
DA,17,ALL,
DA,33,ALL,
DA,49,ALL,

!APPLY GRAVITY LOAD
ACEL,0,0,32.2,

!APPLY PRESSURE FORCE ON SLABS ABOVE GIRDER A1-B1 AND BEAM A1-A2
SFA,85,1,PRES,\\${FORCEX}
SFA,88,1,PRES,\\${FORCEY}

*GET,NUMNODE,KP,621,ATTR,NODE

SOLVE

FINISH

/POST26
NUMVAR,200
LINES,200000
SOLU,199,NCMIT
FILLDATA,199,,,,1,1
REALVAR,199,199
STORE,MERGE
FORCE,TOTAL
```

```
NSOL,2,NUMNODE,U,Y,UY_2
LINES,200000
STORE,MERGE
FORCE,TOTAL

NSOL,3,NUMNODE,U,X,UX_3
LINES,200000
STORE,MERGE
FORCE,TOTAL
PRVAR,2,3
```